BMC Genomics

RESEARCH ARTICLE Open Access

Integration of Genome-Wide Computation DRE Search, AhR ChIP-chip and Gene Expression Analyses of TCDD-Elicited Responses in the Mouse Liver

Edward Dere[1], Raymond Lo[2], Trine Celius[2], Jason Matthews[2] and Timothy R Zacharewski[1,3*]

Abstract

Background: The aryl hydrocarbon receptor (AhR) is a ligand-activated transcription factor (TF) that mediates responses to 2,3,7,8-tetrachlorodibenzo-*p*-dioxin (TCDD). Integration of TCDD-induced genome-wide AhR enrichment, differential gene expression and computational dioxin response element (DRE) analyses further elucidate the hepatic AhR regulatory network.

Results: Global ChIP-chip and gene expression analyses were performed on hepatic tissue from immature ovariectomized mice orally gavaged with 30 μg/kg TCDD. ChIP-chip analysis identified 14,446 and 974 AhR enriched regions (1% false discovery rate) at 2 and 24 hrs, respectively. Enrichment density was greatest in the proximal promoter, and more specifically, within ± 1.5 kb of a transcriptional start site (TSS). AhR enrichment also occurred distal to a TSS (e.g. intergenic DNA and 3' UTR), extending the potential gene expression regulatory roles of the AhR. Although TF binding site analyses identified over-represented DRE sequences within enriched regions, approximately 50% of all AhR enriched regions lacked a DRE core (5'-GCGTG-3'). Microarray analysis identified 1,896 number of TCDD-responsive genes (|fold change| ≥ 1.5, P1(t) > 0.999). Integrating this gene expression data with our ChIP-chip and DRE analyses only identified 625 differentially expressed genes that involved an AhR interaction at a DRE. Functional annotation analysis of differentially regulated genes associated with AhR enrichment identified overrepresented processes related to fatty acid and lipid metabolism and transport, and xenobiotic metabolism, which are consistent with TCDD-elicited steatosis in the mouse liver.

Conclusions: Details of the AhR regulatory network have been expanded to include AhR-DNA interactions within intragenic and intergenic genomic regions. Moreover, the AhR can interact with DNA independent of a DRE core suggesting there are alternative mechanisms of AhR-mediated gene regulation.

Background

The aryl hydrocarbon receptor (AhR) is a ligand activated transcription factor (TF) belonging to the basic-helix-loop-helix-PAS (bHLH-PAS) family of proteins that serve as environmental sensors [1]. 2,3,7,8-Tetrachlorodibenzo-*p*-dioxin (TCDD) is the prototypical AhR ligand, a ubiquitous environmental contaminant that elicits diverse species-specific effects, including tumor promotion, teratogenesis, hepatotoxicity, modulation of endocrine systems, immunotoxicity and enzyme induction [2,3]. These effects result from alterations in gene expression mediated by the AhR [4]. Several studies have demonstrated the requirement for the AhR in mediating TCDD-elicited responses. For example, mice carrying low-affinity AhR alleles are less susceptible to the effects elicited by TCDD [5]. Additionally, AhR-null mice fail to induce responses typically observed following treatment with TCDD and related compounds [6].

TCDD binding to the cytosolic AhR results in a conformational change and translocation to the nucleus. The activated AhR complex heterodimerizes with the aryl hydrocarbon nuclear translocator (ARNT), another

* Correspondence: tzachare@msu.edu
[1]Department of Biochemistry & Molecular Biology, Michigan State University, East Lansing, MI, 48824, USA
Full list of author information is available at the end of the article

bHLH-PAS family member, and binds dioxin response elements (DREs) containing the substitution intolerant 5'-GCGTG-3' core sequence to regulate changes in gene expression [4,7]. Computational searches for all DRE cores in the human, mouse and rat genome identified the highest density of DREs proximal to a transcriptional start site (TSS) [8]. However, a significant number of DRE cores and putative functional DREs have been identified in distal regions within non-coding intergenic segments of the genome. It has been proposed that enrichments for other TFs on outlying regions may be functionally relevant through tertiary looping of genomic DNA and/or via protein tethering mechanisms [9].

The role of specific transcriptional regulators has been studied on a gene-by-gene basis, primarily focusing on regions proximal to the TSS. However, the coupling of chromatin immunoprecipitation with either genomic tiling microarrays (ChIP-chip) or next-generation sequencing (ChIP-seq) has facilitated genome-wide analysis of protein-DNA interactions for a variety of receptors [10-16], TFs [17-20] and components of the basal transcriptional machinery [10,21,22]. Genome-wide location analyses further suggest that TF binding at *cis*-regulatory enhancers in intergenic DNA regions of the genome may also have functional significance [10,17,23,24].

Several studies have investigated AhR-mediated gene expression responses using various technologies [25-30]. Although AhR-DNA interactions have primarily focused on the regulation of *CYP1A1* [4,31], recent global ChIP studies have extended our knowledge of AhR-DNA interactions by examining promoter region binding profiles using *in vitro* and *in vivo* models [32-35] (Lo *et al*., in submission). Our study provides a comprehensive analysis by examining TCDD-induced AhR binding across the entire mouse genome. In addition, we examined AhR binding within chromosomes, intragenic and intergenic DNA regions, and in specific genic regions (i.e., 10 kb upstream of a TSS, 5' and 3' untranslated regions [UTRs], coding sequence [CDS]). Global AhR enrichment data are also integrated with computational DRE core analysis [8], and complementary whole-genome gene expression profiling to provide a more comprehensive evaluation of the hepatic AhR regulatory network elicited by TCDD.

Results

Identification and Characterization of TCDD-Elicited AhR Enrichment

In order to identify regions of AhR enrichment induced by TCDD across the genome, ChIP-chip assays were performed using hepatic tissue from immature ovariectomized mice orally gavaged with 30 μg/kg TCDD for 2 and 24 hrs. CisGenome [36] analysis identified 22,502 and 12,677 enriched regions at 2 and 24 hrs, respectively. Applying a conservative FDR of 0.01 resulted in 14,446 and 974 significant AhR enriched regions at 2 and 24 hrs, respectively (Additional Files 1 and 2 provides a complete list of enriched regions). Ligand activation of the AhR *in vivo* triggers its own rapid degradation and causing a significant reduction of AhR levels [37,38]. This is reflected in the significantly lower number of TCDD-induced AhR enriched regions at 24 hrs as compared to 2 hrs. The distribution, location and enrichment values for each tiled probes across the *Cyp1a1* gene (represented by RefSeq sequences NM_009992 and NM_001136059) are summarized in Figure 1. MA value plots visualize the profile of the enriched region and $\log_2$ fold-enrichment values for each probe are also illustrated (Figure 1). Note that the probes are unevenly tiled throughout the genome, resulting in gaps in genome coverage that may coincide with DRE core locations that may affect AhR enriched region identification. For example, two enriched regions were associated with *Cyp1a1* (Figure 1, red bars). However, the MA plots for 2 and 24 hrs suggest that there is only one large region of enrichment divided into two as a result of the uneven tiling. Consequently, uneven tiling and the lack of tiling in regions that contain DREs may affect the estimated number of AhR enriched regions.

Genomic regions with significant AhR enrichment were mapped to intragenic (10 kb upstream of a TSS plus the transcribed gene of mature RefSeq sequences) and non-coding intergenic regions (Table 1; Additional File 3). Most regions were enriched 5.7-fold with values ranging from 1.7- to 111.4-fold (Figures 2A-B). Enriched regions varied in width from 108 to 6,990 bp (Figure 2C) with 90.5% spanning ≤ 1,500 bp. There was no correlation between fold enrichment and region width (data not shown). Of the 974 significantly enriched regions at 24 h 899 of them overlapped with a 2 hr enriched region (Figure 2D), consistent with reports of constant shuttling of the AhR between the nucleus and cytoplasm [39], and AhR promoter occupancy of targeted genes in untreated cells [34]. Relaxing the FDR to 0.05 increased the overlap to 906, while reducing the number of 24 hr specific enriched regions to 68. Comparable overlaps were identified in promoter-specific ChIP-chip studies of TCDD-induced AhR enrichment at 2 and 24 hrs in the livers of intact C57BL/6 mice, which identified 1,397 number of genes with 403 overlap (Lo *et al*., in submission). Further analysis of the 899 enriched regions found that the fold enrichment values from both time points were positively correlated (Pearson correlation coefficient = 0.4853, two-tailed p-value < 0.0001; Figure 2E).

Although only 40% of the mouse genome consists of intragenic DNA, 71.8% and 64.7% of all sites with significant AhR enrichment at 2 hrs and 24 hrs, respectively, were within this region. The density of AhR enrichment (per million base pairs [Mbp]) was calculated across the entire genome in order to consider the cumulative

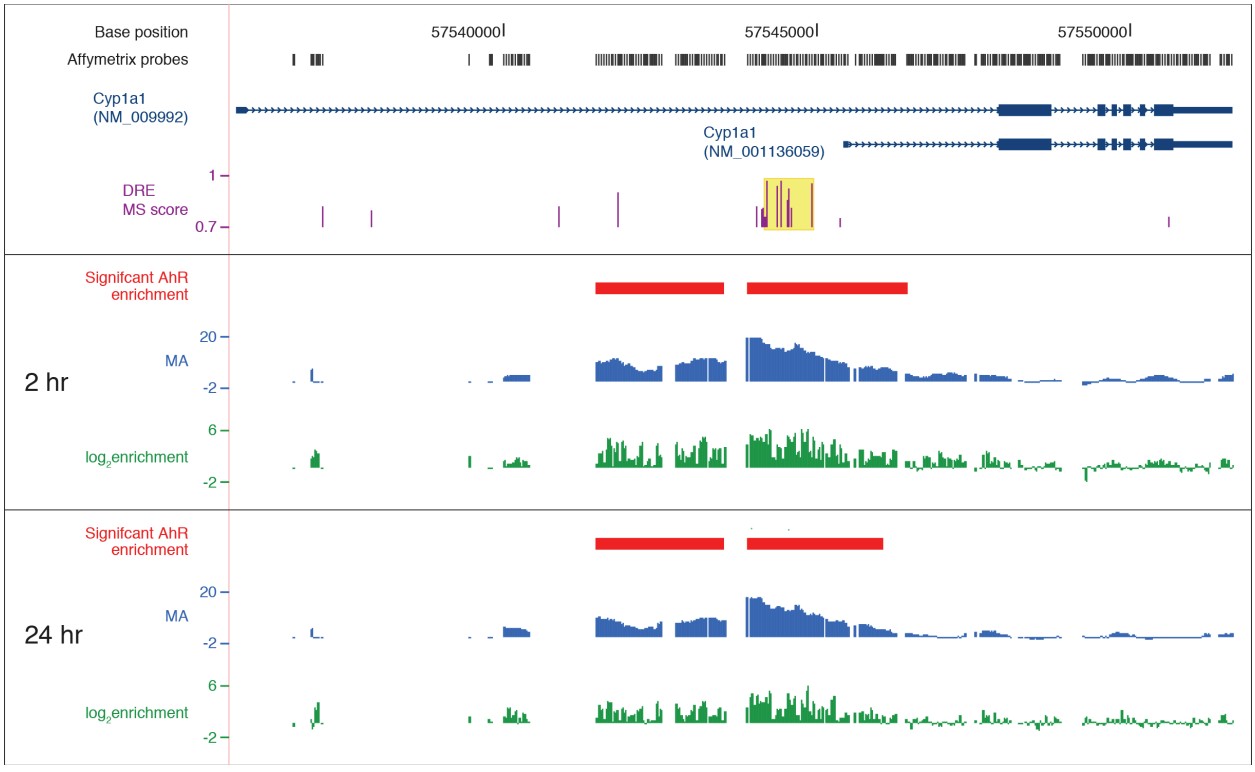

Figure 1 Summary of AhR enrichment within *Cyp1a1* genic region at 2 and 24 hrs. *Cyp1a1* is represented by two RefSeq sequences (NM_009992 and NM_001136059, dark blue tracks) that have different TSSs (dark blue box at far left). The rectangles and lines represent exons and introns, respectively, and the UTRs are depicted as the thinner rectangles. Arrowhead direction indicates the orientation of the gene. The grey boxes above represent the Affymetrix 2.0R mouse tiling array probe locations across the *Cyp1a1* genic regions. The location and matrix similarity (MS) scores of the consensus DREs are represented by the purple histogram. The highlighted yellow box identifies *bona fide* functional DREs (matrix similarity (MS) score ≥ 0.8473) involved in AhR-mediated *Cyp1a1* gene expression. The red boxes identify regions of significant AhR enrichments (FDR < 0.01) based on the moving average (MA) profile by TileMap. The green histogram plots the $\log_2$ fold enrichment values for each individual probe.

intergenic and intragenic DNA region lengths (Table 1). Genome and chromosomal analyses (Additional Files 4 and 5) revealed increased enrichment within intragenic regions compared to non-coding intergenic regions further illustrating a bias for gene encoding regions. However, these values may be inflated due to incomplete probe coverage in the intergenic regions and sequence gaps in the genome. Specific analysis of the 10 kb upstream, 5' and 3' UTRs and CDS regions revealed the highest density of AhR enrichment was proximal to the TSS (Table 1 and Additional Files 4 and 5). AhR enrichment density was greatest within ± 1.5 kb at 2 and 24 hrs (Figures 3A-B), coinciding with proximal promoter DRE core densities [8] and RNA polymerase II binding at the TSSs [10]. Interestingly, there is a notable cleft in AhR enrichment 200 bp directly upstream and downstream of the TSSs, possibly to accommodate general transcription machinery. Both global and

Table 1 Distribution and density analysis of TCDD-induced AhR enriched regions[a] in the mouse genome

					Genic Region[c]			
		Genome	Intergenic DNA[b]	Intragenic DNA[b]	10kb upstream	5' UTR	CDS	3' UTR
2 hr	AhR enrichment	14,446	4,163	10,283	4,601	2,569	7,499	225
	Enrichment density[d]	5.44	2.62	9.64	18.65	17.29	7.21	7.29
24 hr	AhR enrichment	974	344	630	306	132	507	9
	Enrichment density[d]	0.37	0.22	0.59	1.24	0.89	0.49	0.29

[a] AhR enriched regions with a FDR < 0.01

[b] intergenic, intragenic and gene regions are defined as previously described in Additional File 1

[c] regions are defined using the genomic locations in the refGene database from the UCSC Genome Browser

[d] density calculated per million base pairs

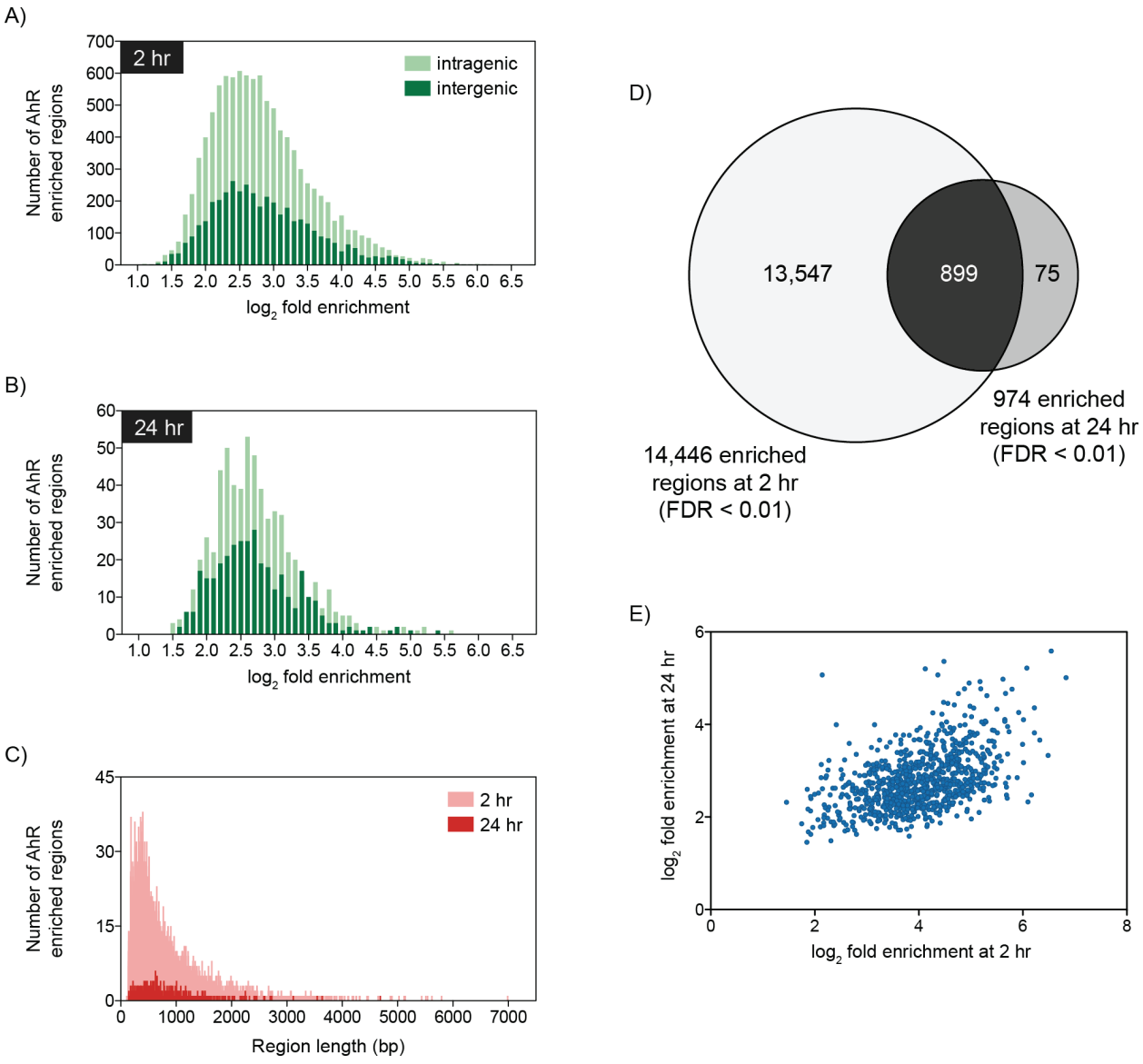

Figure 2 Characterization of TCDD-induced AhR enriched regions at 2 and 24 hrs (FDR < 0.01). Frequency analysis of enriched regions relative to $\log_2$ fold enrichment at 2 hr (**A**) and 24 hr (**B**) illustrating enrichment values in intragenic (light green) and intergenic (dark green) DNA regions. Distribution of enriched regions relative to region width (**C**) at 2 hrs (light red) and 24 hrs (dark red) identified 90.5% of enriched sites were ≤ 1,500 bp. Comparison of AhR enriched regions at 2 and 24 hrs identified 899 overlapping regions (**D**). Analysis of the fold enrichment values for the 899 overlapping regions at 2 and 24 hrs identified a positive correlation (two-tailed P-value < 0.0001, Pearson correlation coefficient = 0.4853; **E**).

proximal promoter density analyses illustrate TCDD-induced AhR enrichments are more prominent in regions directly associated with a gene. Nevertheless, there are a significant number of distally located enrichment sites that may also be functionally relevant.

Confirmation of AhR ChIP-chip Enrichment Analysis

Selected regions of AhR enrichment identified by ChIP-chip analysis at 2 hrs were confirmed by ChIP-PCR (Figure 4). Three representative ChIP-chip enrichments from each genomic region (intergenic, 10 kb upstream of a TSS, 5' UTR, CDS and 3' UTR) were selected to validate AhR enrichments with and without a DRE core at different positions relative to the TSS. ChIP-PCR and ChIP-chip analysis of DRE containing regions exhibited similar levels of AhR enrichment relative to IgG_{TCDD} controls and were significantly greater than vehicle controls relative to $IgG_{vehicle}$. AhR enriched regions without the DRE core were also verified, further demonstrating that the AhR can interact with DNA independent of a

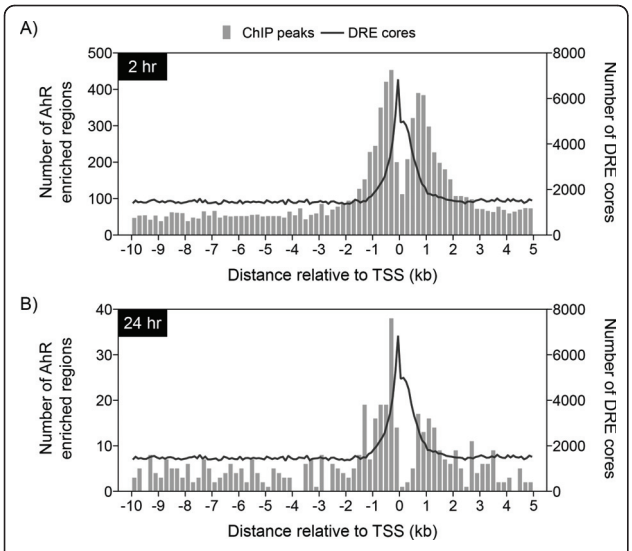

Figure 3 TCDD-induced AhR enrichment (FDR < 0.01) densities in the proximal promoter (10 kb upstream and 5 kb downstream of a TSS) at 2 hrs (A) and 24 hrs (B). The bars represent the number of enriched regions in each 200 bp window. The number of DRE cores in 100 bp non-overlapping windows is superimposed (line) illustrating the overlap between AhR enriched regions and DRE cores in the proximal promoter region.

DRE core, but does not eliminate the possibility of AhR interaction through DNA looping or protein tethering. Interestingly, the fold enrichment values for regions without the DRE core were consistently lower than those with a DRE core, suggesting AhR interactions are stronger in regions containing a DRE.

DRE Analysis of AhR Enriched Regions

TCDD-elicited changes in gene expression are mediated through AhR signaling via binding to the substitution intolerant DRE core sequence (5'-GCGTG-3'). Overlaying TCDD-induced AhR enrichment with DRE core locations throughout the mouse genome [8] identified 57.8% and 48.5% of the enriched regions did not contain a DRE core regions at 2 and 24 hrs, respectively (Table 2 and Figures 5A-B). Other promoter-specific ChIP-chip studies have also reported DRE cores in ~50% of the AhR enriched regions [33,35]. The remaining enriched regions possessed at least one and as many as 16 DRE cores (Table 2). AhR enriched regions with or without a DRE core exhibited similar widths and levels of enrichment.

Matrix similarity (MS) scores have been calculated for each 19 bp DRE sequence within the mouse genome using a position weight matrix (PWM) constructed from *bona fide* functional DREs [8]. Of the 6,595 significant AhR enriched regions containing a DRE core (6,093 from 2 hr and 502 from 24 hr), 90.7% were within 500 bp of a DRE core (i.e. distance of maximum enrichment within the region to an underlying DRE core) with half of these positions located within 135 bp of a DRE core. However, only 8.3% and 17.8% of the AhR enriched regions at 2 and 24 hrs, respectively, possessed a putative functional (high scoring) DRE sequence (MS score ≥ 0.8473) suggesting the AhR may bind other degenerate sequence elements.

AhR binding to an alternate response element (5'-$CATGN_6C[T|A]TG$-3') has also been reported [40,41]. Of the 8,353 and 472 enriched regions at 2 and 24 hrs, respectively, that did not contain a DRE core, 482 and 237, respectively, contained the alternate DRE sequence (5.8% and 50.2%, respectively). The higher incidence of AhR enriched regions at 24 hrs containing the alternate response element may represent tertiary AhR binding sites resulting from conformational changes and crowding of the promoter with the general transcription machinery [42,43].

Transcription Factor Binding Site Over-Representation Analysis

Significantly AhR enriched regions were computationally analyzed for over-represented response elements for known TF binding site (TFBS) families using RegionMiner (Genomatix). DREs as well other sites for early growth response (EGR), E2F, nuclear respiratory factor 1 (NRF1), nuclear receptor subfamily 2 factors (NR2F/COUP-TF) and peroxisome proliferator-activated receptor (PPAR) were over-represented within AhR enriched regions (Table 3; complete list of over-represented TFBS are provided in Additional Files 6 and 7). Many of these TF sites were enriched proximally to a DRE core (i.e. within 10-50 bp; Additional File 8) suggesting possible interactions. Studies have previously reported interactions between AhR and many of these TFs [34,44,45]. For example, AhR complexes with EGR-1 following treatment of human HUVEC cells with high glucose concentrations [45]. In addition, AhR aggregates with E2F1 to inhibit E2F1-induced apoptosis [46]. AhR also directly interacts with COUP-TF to repress ER-mediated gene expression [47].

De Novo Motif Analysis

Approximately 50% of enriched regions lacked the DRE core sequence (Figures 5A-B) suggesting AhR interacts with DNA using alternate strategies. *De novo* motif analysis of these regions using the Gibbs motif sampler in CisGenome identified over-representation of comparable repetitive elements in both the intergenic and intragenic DNA regions (Additional File 9). Comparison of over-represented non-repetitive motifs to existing TF binding motifs in JASPAR and TRANSFAC [48,49] using STAMP [50] identified similarities to COUP-TF, hepatocyte nuclear factor 4 (HNF4), liver receptor homolog 1 (LRH1/NR5A2) and PPAR binding sites (Figure 6). Interestingly, COUP-TF and HNF4 belong to the NR2F

A)

List of AhR enriched regions[a] identified by ChIP-chip analysis at 2 hrs confirmed by ChIP-PCR. Three representive enrichments with and without a DRE core were chosen from each genomic region.

Enrichment ID	Genomic region	DRE[b]	Gene Symbol	RefSeq	Enrichment ID	Genomic region	DRE[b]	Gene Symbol	RefSeq
AhR_106					AhR_82				
AhR_129	Intergenic	yes	NA	NA	AhR_159	Intergenic	no	NA	NA
AhR_130					AhR_216				
AhR_1			Cyp1a1	NM_009992	AhR_4			Slc35d1	NM_177732
AhR_2	10 kb upstream	yes	Tiparp	NM_178892	AhR_35	10 kb upstream	no	Pcp4l1	NM_025557
AhR_11			Cyp1b1	NM_009994	AhR_1456			Cyp1a1	NM_009992
AhR_196			Myo1b	NM_010863	AhR_51			Bach2	NM_007521
AhR_198	5' UTR	yes	Edc3	NM_153799	AhR_581	5' UTR	no	Atxn1	NM_009124
AhR_507			Sfxn1	NM_027324	AhR_857			Tbc1d16	NM_172443
AhR_21			Prom1	NM_008935	AhR_146			Npc1	NM_008720
AhR_151	CDS	yes	Pkm2	NM_011099	AhR_201	CDS	no	Derl1	NM_024207
AhR_236			Lmo7	NM_201529	AhR_908			Erbb3	NM_010153
AhR_476			AI464131	NM_001085515	AhR_143			Rbm4	NM_009032
AhR_714	3' UTR	yes	Irf2bp2	NM_001164598	AhR_3220	3' UTR	no	Irs1	NM_010570
AhR_907			Wipf3	NM_001167860	AhR_5515			Cebpa	NM_007678

[a] AhR enriched regions at 2 hrs with FDR < 0.01
[b] 5′-GCGTG-3′ core DRE sequence
NA: Not applicable

B)

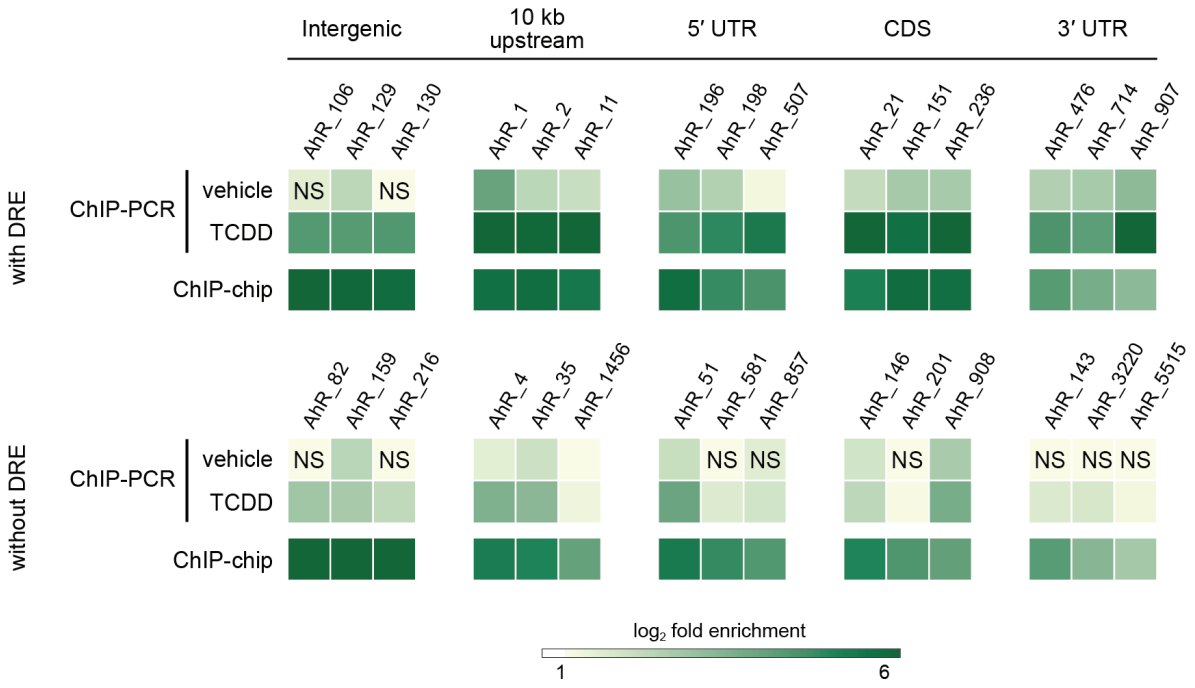

Figure 4 Confirmation of hepatic TCDD-induced AhR enrichment identified by ChIP-chip analysis (FDR < 0.01) at 2 hrs by ChIP-PCR. Selected regions were chosen for verification based on position relative to a TSS, ChIP-chip fold enrichment and the presence or lack of a DRE core within the region of enrichment (**A**). Immunoprecipitated DNA was measured by QRTPCR and AhR enrichment was calculated as fold induction above IgG controls. The color intensity of each box represents the mean value of three independent replicates. NS = not significant compared to IgG controls ($p < 0.05$). 2 hr ChIP-chip enrichment values are provided in Additional File 1.

family identified in the TFBS over-representation analysis of all AhR enriched regions (Table 3). The presence of these binding motifs in non-DRE containing regions of AhR enrichment further suggests that AhR-DNA interactions occur through a tethering mechanism involving other TFs or by tertiary looping of DNA.

Table 2 Distribution of DRE cores in AhR enriched regions[a]

Number of DRE cores[b]	Number of AhR enriched regions	
	2 hr	24 hr
0	8,353	472
1	3,705	289
2	1,372	121
3	544	46
4	223	16
5	109	12
6	67	7
7	25	5
8	15	0
9	11	3
10	7	1
11	5	0
12	3	1
13	0	0
14	3	1
15	3	0
16	1	0
Total	**14,446**	**974**

[a] AhR enriched regions with a FDR < 0.01

[b] 5'-GCGTG-3' core sequence

Gene Level Analysis of AhR Enrichment

Of the 10,369 enrichments identified in the intragenic DNA regions, 43.8% (4,544/10,369) contained a DRE core at 2 hrs, and 52.4% (332/634) at 24 hrs (Figure 5, areas shaded blue). These intragenic AhR enriched regions mapped to 5,307 and 591 unique genes at 2 and 24 hrs, respectively (AhR targeted genes are provided as gene annotated enriched regions in Additional Files 1 and 2). Molecular and cellular functional analysis using Ingenuity Pathway Analysis (IPA) found these genes to be associated with lipid and carbohydrate metabolism, small molecule biochemistry, cell cycle and gene expression based on a Fisher's Exact Test p-value < 0.01 (Figure 7; Additional Files 10 and 11 list the most significant over represented biological functions at 2 and 24 hrs). Furthermore, 63.5 and 56.2% of the genes associated with AhR enrichment at 2 and 24 hrs, respectively, contained a DRE core within the region of enrichment (Figure 8). The higher percentage of genes containing a DRE core compared to enriched regions with a DRE core is due to multiple regions of AhR enrichment associated with a single gene (as illustrated for *Cyp1a1* in Figure 1). The remaining genes (36.5% and 54.8% at 2 and 24 hrs, respectively) with significant AhR enrichment were targeted independently of a DRE core.

At both 2 and 24 hrs, 575 genes had AhR enrichment, with 513 possessing DRE cores in the AhR enriched region (Figure 8C). Only 16 genes exhibited AhR enrichment solely at 24 hrs, with three containing a DRE core. In contrast, 4,732 genes possessed significant AhR enrichment with 60.4% (2,856) containing a DRE core within the region of enrichment at 2 hrs. Due to the large overlap of enriched regions at 2 and 24 hrs, the remaining analysis focuses predominantly on the AhR enrichment at 2 hr.

Comparison of Transcriptional Responses with AhR Enrichment

Gene expression analysis at 2, 4, 8, 12, 18, 24, 72, and 168 hrs identified 1,896 unique differentially expressed genes (|fold change| ≥ 1.5 and P1(t) > 0.999) at one or more time points. Of the 1,896 TCDD-responsive genes, 900 genes (47.5%) possessed significant AhR enrichment within the intragenic region (10 kb upstream of the TSS to the end of the transcript). Moreover, of the 900 genes exhibiting AhR enrichment at 2 hrs, 625 contained a DRE core sequence, suggesting these responses are AhR-mediated. The remaining 275 differentially expressed genes were not associated with a AhR enriched region containing a DRE core, and may be secondary responses. In order to concisely visualize the integration of the DRE, ChIP-chip and gene expression analyses, Circos plots were generated for the genome and individual chromosomes (Figure 9 and Additional File 12). The plots further illustrate the diversity in AhR enrichment locations in relation to the genomic position of dysregulated genes. Further analysis of the responsive genes found that most were induced by TCDD (Table 4) at all time points. Greater than 82% of the induced genes at 2 or 4 hrs had significant AhR enrichment, and more than 62% of them contained at least one DRE core suggesting that regulation is DRE-dependent fashion. In contrast, only 35% of the 691 genes induced at 168 hrs, exhibited AhR enrichment with 26% possessing a DRE core suggesting that these are secondary gene expression responses. Interestingly, down-regulated genes associated with AhR enrichment were relatively consistent across all time points. Approximately one third of the down-regulated genes appear to be AhR regulated with DRE involvement.

Functional analysis of the 900 differentially expressed genes associated with AhR enrichment was performed using DAVID [51]. The most over-represented functions were associated with lipid metabolic processes (enrichment score of 7.34, Table 5), consistent with the induced fatty liver phenotype [52,53]. IPA analysis of these genes also identified lipid metabolism as an enriched molecular and cellular function (Fisher's Exact Test p-value < 0.01; Figure 10; Additional File 13 provides a list of the most significant biological functions). In addition, *de novo* motif analysis (Figure 6) identified binding sites for TFs associated with lipid metabolism and transport. The

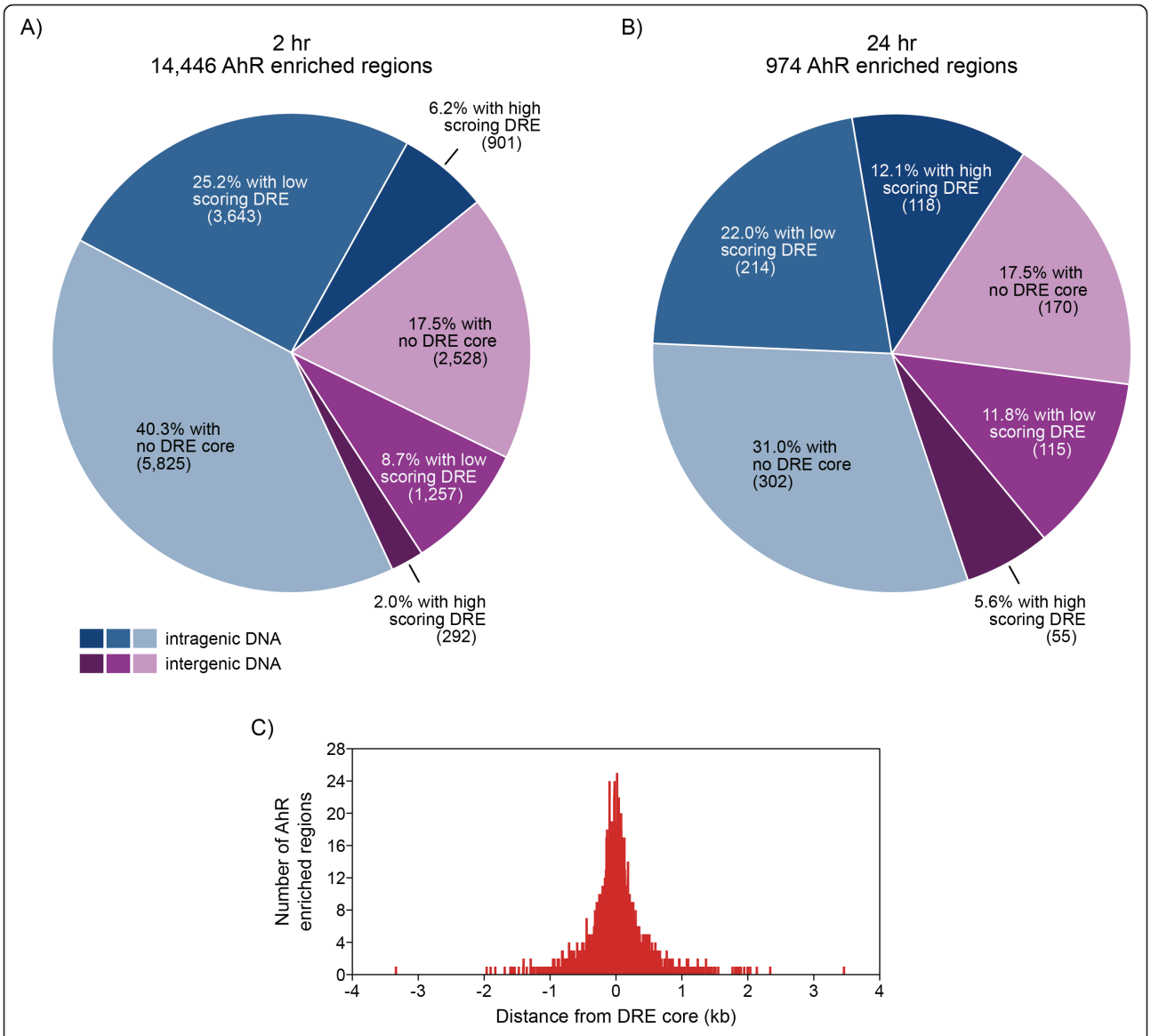

Figure 5 Mapping TCDD-induced AhR enriched regions (FDR < 0.01) with DRE locations. Regions of enrichment identified in the intergenic (purple) and intragenic (blue) DNA regions of the genome at 2 hrs (**A**) and 24 hrs (**B**) were searched for high scoring (putative functional) DRE sequences (matrix similarity score ≥ 0.8473; dark blue and dark purple segments) and low scoring DRE sequences (matrix similarity score < 0.8473; mid blue and mid purple segments) using a position weight matrix developed from *bona fide* functional DREs [8]. Light blue and light purple segments represent regions with no DRE core sequence. A total of 6,595 enriched regions (6,093 at 2 hrs and 502 at 24 hrs) contained at least one DRE core (5'-GCGTG-3'). 50% of these regions were within 135 bp of a DRE core (based on the location of maximum enrichment within the enriched region; **C**).

induction of AhR regulated xenobiotic enzymes, such as cytochrome P450s, glutathione S-transferases (Gsts) and UDP-glucuronosyltransferases (Ugts), hallmarks of TCDD exposure, were also identified as an enriched cluster (enrichment score of 3.54).

Although AhR mediates the expression of enzymes involved in xenobiotic metabolizing enzymes, including NADP(H) dehydrogenase, quinone 1 (*Nqo1*) and UDP-glucose dehydrogenase (*Ugdh*) as well as several Ugt and Gst isoforms, they are also regulated by nuclear factor, erythroid derived 2, like 2 (Nrf2) via antioxidant response elements in response to oxidative stress [54,55]. Recent studies with AhR and Nrf2 null mice report that TCDD induction of *Nqo1* is AhR and Nrf2 dependent [56]. Furthermore, specific Ugt and Gst isoforms induced by TCDD require Nrf2. Collectively, these responses are referred to as the "TCDD-inducible AhR-Nrf2 gene battery." ChIP-chip and gene expression

Table 3 Significantly over-represent transcription factor module families in TCDD-induced AhR enriched regions[a]

TF Module Family	Module Description	2 hr AhR enriched regions				24 hr AhR enriched regions			
		# of matches	Expected # of matches	Over-representaion[b]	Z-Score	# of matches	Expected # of matches	Over-representaion[b]	Z-Score
AHR	AhR-ARNT heterodimer	9,447	4,278.30	2.21	79.03	851	297.44	2.86	32.07
SP1	GC-Box factors SP1/GC	19,356	12,839.04	1.51	57.54	1,346	892.61	1.51	15.17
HIF	Hypoxia inducible factor, bHLH/PAS protein family	8,763	4,841.13	1.81	56.37	569	336.57	1.69	12.64
E2F	E2F-Myc activator/cell cycle regulator	18,247	12,444.88	1.47	52.04	1,266	865.21	1.46	13.62
ZBP	Zinc binding protein factors	25,542	18,518.20	1.38	51.65	1,739	1,287.45	1.35	12.58
NRF1	Nuclear respiratory factor 1	3.475	1,494.81	2.32	51.21	252	103.92	2.42	14.48
ZF5	ZF5 POZ domain zinc finger	3,156	1,442.92	2.19	45.09	205	100.32	2.04	10.40
NF1	Nuclear factor 1	13,047	8,876.90	1.47	44.27	886	617.15	1.44	10.81
NR2F	Nuclear receptor subfamily 2 factors	44,774	36,390.64	1.23	44.02	3,180	2,530.00	1.26	12.93
EGR	EGR/nerve growth factor included protein c	22,224	16,794.62	1.32	41.92	1,541	1,167.62	1.32	11.
PPAR	Peroxisome proliferator-activated receptor	24,808	19,035.70	1.30	41.87	1,752	1,323.43	1.32	11.78
RXR	RXR heterodimer binding sites	41,027	33,441.00	1.23	41.54	2,932	2,324.93	1.26	12.60
WHN	Winged helix binding sites	3,030	1,477.23	2.05	40.39	206	102.70	2.01	10.14

[a] AhR enriched regions with a FDR < 0.01

[b] total number of matches in enriched regions/expected number of matches in genome

Complete list of over-represented TF module families are provided in Additional Files 6 and 7

analysis indicates that *Nqo1*, *Gstm1*, *Gstm2*, *Ugdh* and *Nrf2* induction is associated with AhR enrichment. Although supportive of the Nrf2-dependency model, these data do not distinguish if these are secondary responses mediated by Nrf2 alone, or involve an AhR-Nrf2 interaction. In contrast, *Gsta1* and *Ugt2b35* induction occurred independently of AhR enrichment, suggesting they may only be dependent on Nrf2 [56].

Immune cell accumulation following a single acute dose of TCDD at 168 hrs is presumed to be a secondary

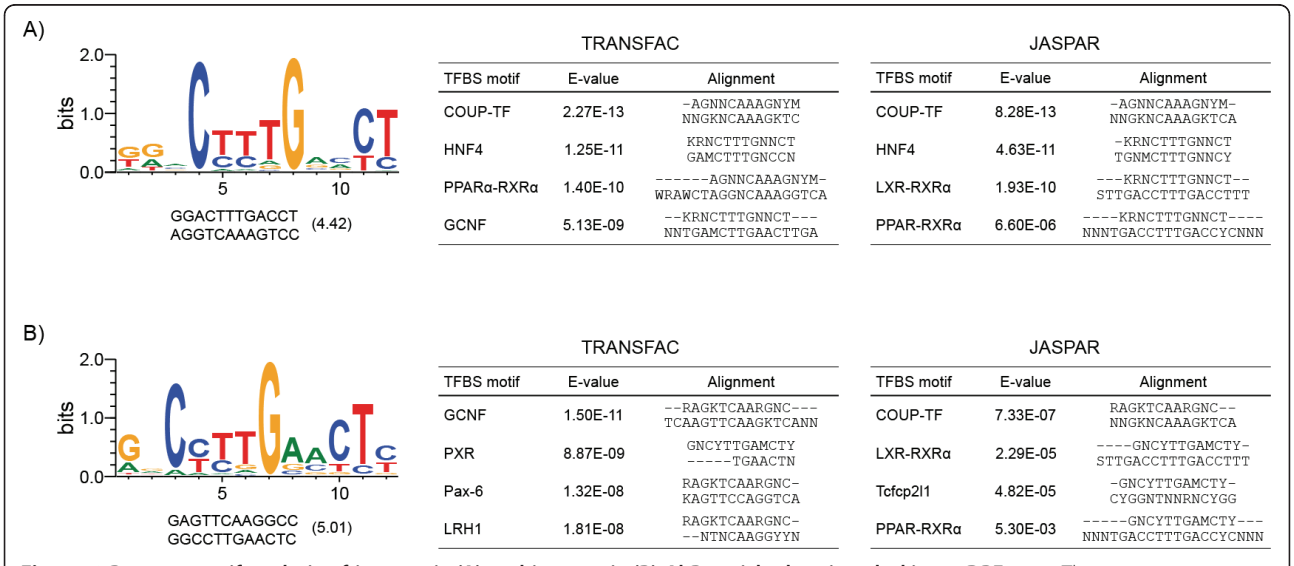

Figure 6 *De novo* motif analysis of intragenic (A) and intergenic (B) AhR enriched regions lacking a DRE core. The non-repetitive over-represented motifs from each region are shown with their consensus and reverse complement sequence, and the Gibbs motif sampler score. Over-represented motifs were associated with specific TFBSs in JASPAR and TRANSFAC based on the consensus sequence alignments and E-value scores.

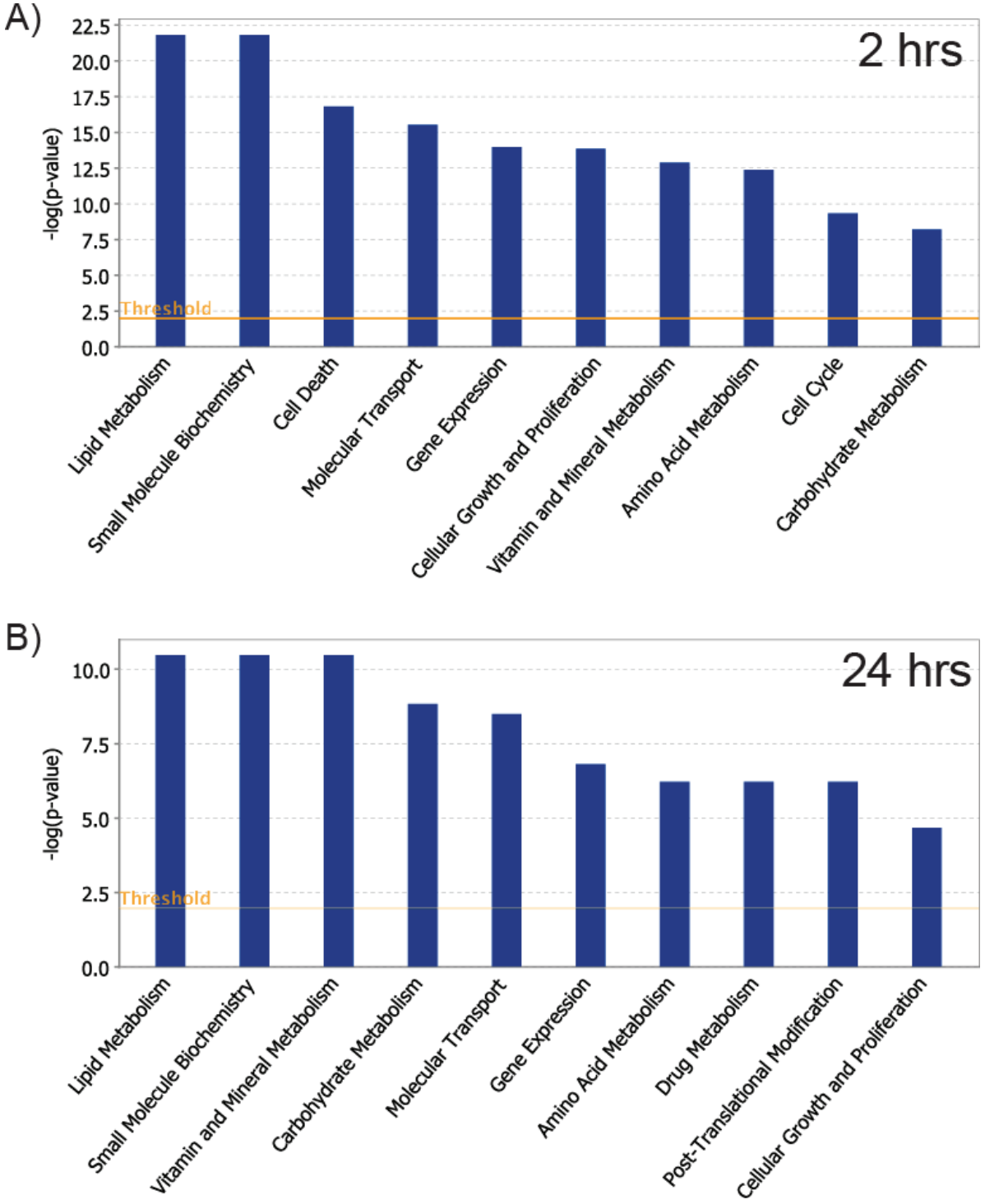

Figure 7 Molecular and cellar functions over-represented by genes associated with significant AhR enrichment (FDR < 0.01) containing a DRE core. The 4,544 and 332 unique genes with AhR enrichment with a DRE core at 2 hrs (**A**) and 24 hrs (**B**), respectively, were analyzed using Ingenuity Pathway Analysis for enriched biological functions using Fisher's Exact Test ($p < 0.01$; orange line). The blue bars represent the log Odds value calculated from the p-value of each functional group.

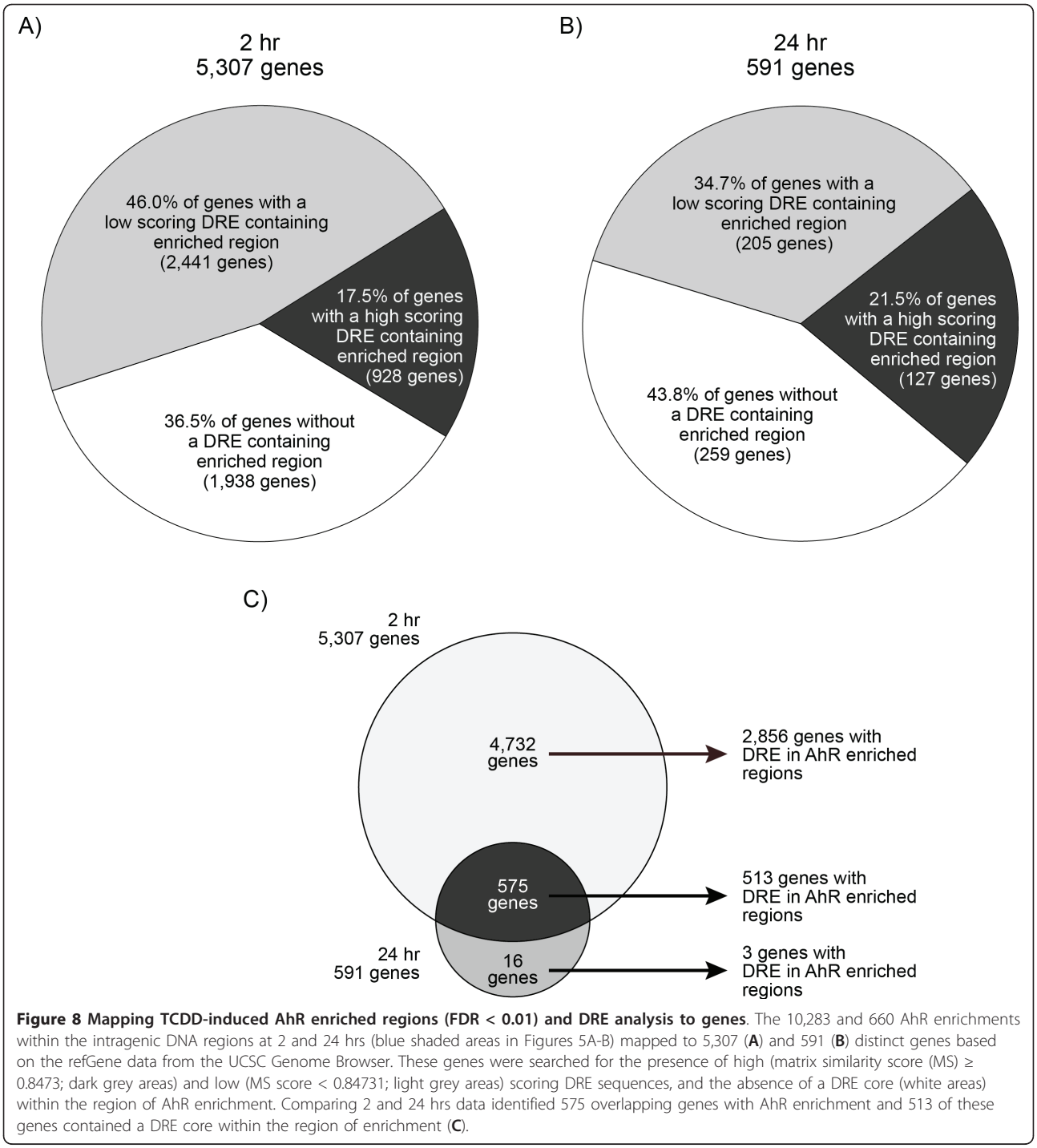

Figure 8 Mapping TCDD-induced AhR enriched regions (FDR < 0.01) and DRE analysis to genes. The 10,283 and 660 AhR enrichments within the intragenic DNA regions at 2 and 24 hrs (blue shaded areas in Figures 5A-B) mapped to 5,307 (**A**) and 591 (**B**) distinct genes based on the refGene data from the UCSC Genome Browser. These genes were searched for the presence of high (matrix similarity score (MS) ≥ 0.8473; dark grey areas) and low (MS score < 0.84731; light grey areas) scoring DRE sequences, and the absence of a DRE core (white areas) within the region of AhR enrichment. Comparing 2 and 24 hrs data identified 575 overlapping genes with AhR enrichment and 513 of these genes contained a DRE core within the region of enrichment (**C**).

response to hepatic injury or fatty acid accumulation [52,53]. DAVID analysis of genes induced at 168 hrs identified multiple over-represented immune-related clusters (enrichment scores > 2). However, several of the genes including complement component 1, q subcomponent, beta polypeptide (*C1qb*), CD36 antigen (*Cd36*), complement component 4A (C4a) and interferon regulatory factor 8 (Irf8), did not exhibit accompanying AhR enrichment within their intragenic region (10 kb upstream of the TSS to the end of the 3' UTR). Only 26 out of 105 differentially regulated genes in the enriched immune clusters exhibited AhR enrichment. Collectively, these data suggest that gene expression associated with immune function is a consequence of immune cell infiltration into the liver.

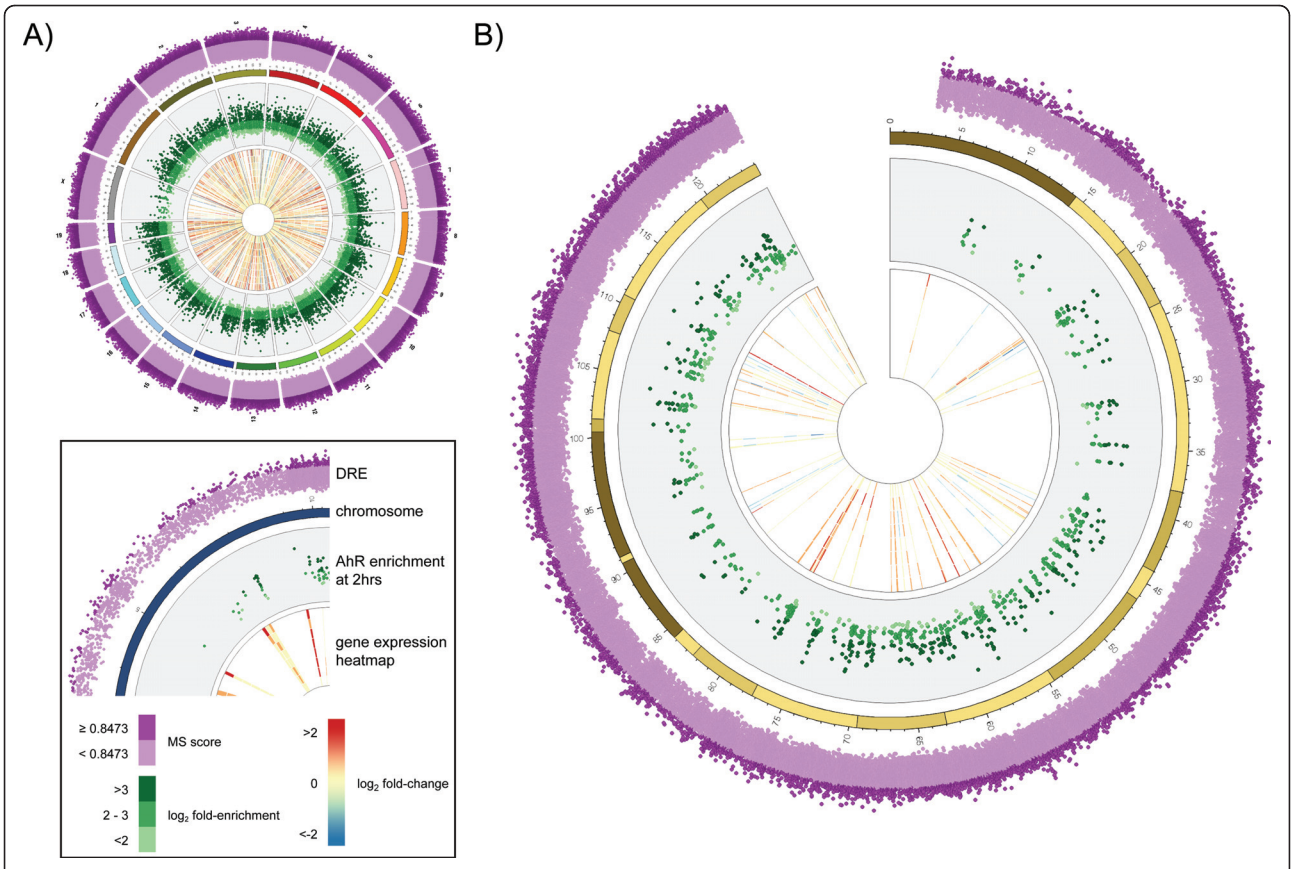

Figure 9 Circos plots integrating DRE analysis, AhR enrichment (2 hrs; FDR < 0.01) and heatmaps for hepatic differential gene expression responses (|fold change| ≥ 1.5 and P1(t) > 0.999) induced by TCDD across the genome (A) and chromosome 9 (B). The inset legend image provides information represented by each data ring. DRE matrix similarity (MS) scores and AhR enrichment values increase radially outward. The time points for the gene expression heatmaps also increase radial outward. The arc of each heatmap wedge maps directly to the location of the gene in the genome. The arc length is proportional to the length of the transcribed region. Circos plots for the other chromosomes are provided in Additional File 12.

Discussion

This study further elucidates the role of the AhR in mediating the hepatic effects of TCDD in C57BL6 mice. Recent studies have mapped AhR binding using promoter-focused ChIP-chip arrays and found that ~50% of the AhR enriched regions were devoid of the DRE core [32-34]. The lack of a DRE core in regions of AhR enrichment was also reported in a AhR

Table 4 Distribution and AhR enrichment and DRE analysis of differentially expressed genes elicited by TCDD

			2 hr	4 hr	8 hr	12 hr	18 hr	24 hr	72 hr	168 hr
Number of differentially expressed genes[a]	Up-regulated	Total	68	255	341	218	236	287	267	719
		With AhR enrichment[b]	55	200	202	148	172	186	164	243
		With AhR enrichment[b] + DRE core[c]	47	168	171	126	146	156	135	181
	Down-regulated	Total	18	233	116	168	105	237	261	218
		With AhR enrichment[b]	10	123	76	102	59	131	137	123
		With AhR enrichment[b] + DRE core[c]	6	79	49	63	30	72	79	70

[a] |fold-change| ≥ 1.5 and P1(t) > 0.999

[b] AhR enriched regions at 2 hrs with FDR < 0.01

[c] 5'-GCGTG-3' core sequence within AhR enriched region

Table 5 Functional enrichment analysis of differently regulated[a] genes with AhR enrichment[b] using DAVID

Category	Team	Gene Count	Fold enrichment	P-value
Enrichment Score: 7.34				
GOTERM_BP_3	GO:0006629 ~ lipid metabolic process	76	2.23	5.53E-11
GOTERM_BP_3	GO:0044255 ~ cellular lipid metabolic process	53	2.23	7.80E-08
GOTERM_BP_3	GO:0008610 ~ lipid biosynthetic process	32	2.30	2.28E-05
Enrichment Score:4.12				
GOTERM_BP_3	GO:0048523 ~ negative regulation of cellular process	94	1.60	4.46E-06
GOTERM_BP_3	GO:0048519 ~ negative regulation of biological process	101	1.54	7.83E-06
GOTERM_BP_3	GO:0031324 ~ negative regulation of cellular metabolic process	45	1.85	8.99E-05
GOTERM_BP_3	GO:0051172 ~ negative regulation of nitrogen compound metabolic process	39	1.96	9.68E-05
GOTERM_BP_3	GO:0009890 ~ negative regulation of biosynthetic process	40	1.86	2.33E-04
GOTERM_BP_3	GO:0009892 ~ negative regulation of metabolic process	46	1.74	3.20E-04
GOTERM_BP_3	GO:0010605 ~ negative regulation of macromolecule metabolic process	43	1.72	6.88E-04
Enrichment Score: 3.54				
GOTERM_BP_3	GO:0009410 ~ response to xenobiotic stimulus	8	10.59	3.54E-06
GOTERM_BP_3	GO:0006805 ~ xenobiotic metabolic process	7	11.59	1.12E-05
GOTERM_BP_3	GO:0018894 ~ dibenzo-p-dioxin metabolic process	3	19.86	7.31E-03
GOTERM_BP_3	GO:0009404 ~ toxin metabolic process	3	11.92	2.28E-02
Enrichment Score: 2.70				
GOTERM_BP_3	GO:0051272 ~ positive regulation of call motion	9	4.58	6.00E-04
GOTERM_BP_3	GO:0051270 ~ regulation of cell motion	15	2.84	7.55E-04
GOTERM_BP_3	GO:0040017 ~ Positive regulation of locomotion	9	4.26	1.01E-03
GOTERM_BP_3	GO:0030334 ~ regulation of cell migration	13	2.87	1.76E-03
GOTERM_BP_3	GO:0040012 ~ regulation of locomotion	13	2.39	7.93E-03
GOTERM_BP_3	GO:0040012 ~ regulation of localization	32	1.61	9.36E-03
Enrichment Score: 2.55				
GOTERM_BP_3	GO:0048518 ~ positive regulation of biological process	106	1.44	7.45E-05
GOTERM_BP_3	GO:0048522 ~ positive regulation of cellular process	94	1.45	2.03E-04
GOTERM_BP_3	GO:0009893 ~ positive regulation of metabolic process	51	1.53	2.64E-03
GOTERM_BP_3	GO:0010604 ~ positive regulation of macromolecule metabolic process	48	1.54	3.02E-03
GOTERM_BP_3	GO:0031325 ~ positive regulation of cellular	47	1.48	6.67E-03
GOTERM_BP_3	GO:0009891 ~ positive regulation of biosynthetic	38	1.38	3.96E-02
GOTERM_BP_3	GO:0031325 ~ positive regulation of nitrogen compound metabolic process	36	1.39	4.40E-02
Enrichment Score: 2.44				
GOTERM_BP_3	GO:0005996 ~ monosaccharide metabolic process	21	2.27	9.50E-04
GOTERM_BP_3	GO:0005975 ~ carbohydrate metabolic process	37	1.67	2.63E-03
GOTERM_BP_3	GO:0016051 ~ carbohydrate biosynthetic process	11	2.70	7.19E-03
GOTERM_BP_3	GO:0044262 ~ cellular carbohydrate metabolic process	27	1.70	9.34E-03

[a] |fold-change| ≥ 1.5 and P1(t) >0.999 at one or more time points

[b] AhR enriched regions at 2 hrs with FDR < 0.01

genome-wide ChIP-chip study performed in mouse CH12.LX cells [57]. ChIP-seq experiments for other TFs have also demonstrated enrichment in remote genome regions, which may serve important regulatory roles [10,11,14,17]. Collectively these data suggest the AhR uses different mechanisms to regulate gene expression. Moreover, the integration of genome-wide *in silico* DRE search, with *de novo* motif analysis and TCDD-elicited hepatic temporal gene expression data has further elucidated the hepatic AhR gene regulatory network.

ChIP-chip analysis identified 14,446 TCDD-induced AhR regions at 2 hrs and 974 regions at 24 hrs, consistent with the rapid nuclear export and subsequent degradation of the AhR following TCDD activation [37]. Approximately half of these regions were within intragenic regions (10 kb upstream of a TSS to the end of the 3' UTR). Furthermore, 25% of these enriched regions at 2 hrs and 19% at 24 hrs were within 2 kb of a TSS, indicating that a large subset of AhR enrichment occurs adjacent to a TSS. Unlike other studies that report a normal distribution of TF binding centered around the

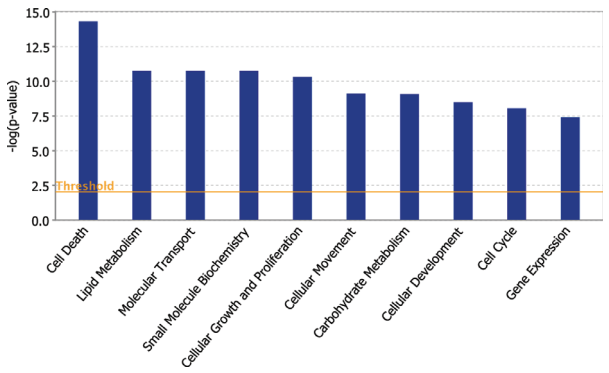

Figure 10 Molecular and cellar functions over-represented by differentially regulated genes (|fold change| ≥ 1.5, P1(t) > 0.999) associated with significant AhR enrichment (FDR < 0.01) at 2 hrs. The 900 differentially regulated genes with AhR enrichment were analyzed using Ingenuity Pathway Analysis for enriched biological functions using Fisher's Exact Test ($p < 0.01$; orange line). The blue bars represent the log Odds value calculated from the p-value of each functional group.

TSS [15,58-60], the AhR density profile exhibited a cleft immediately adjacent to the TSS, possibly to accommodate recruited transcriptional machinery.

Although most AhR enrichment regions are intragenic, a significant number are located in distal intergenic regions (i.e. 4,163 of 14,446 at 2 hrs and 344 of 974 at 24 hrs). Studies with the ER, p53 and forkhead box protein A1 [10,11,14,17] suggest distal TF binding may have distinct regulatory roles. Binding proximal to the TSS is presumed to stabilize the general transcriptional machinery, while distal binding regulates transcription by a looping mechanism or by altering chromatin structure [9,61,62]. Consequently, AhR binding outside of the proximal promoter region may have important regulatory roles that remain largely uninvestigated.

Comparing AhR enriched regions with DRE cores revealed that their intergenic, intragenic and genic (10 kb upstream, UTRs, and CDS) density distributions were similar. The greatest density of AhR enrichment associated with a DRE core occurred within the proximal promoter. Both exhibited comparable distribution profiles except for the cleft in enrichment at the TSS. The decrease in AhR enrichment at the TSS coincides with RNA polymerase II binding at the TSSs [10] of transcriptionally responsive genes. Although TCDD-elicited differential gene expression is thought to be mediated by the substitution intolerant DRE core sequence (5'-GCGTG-3'), only ~50% of the AhR enriched regions contained a DRE core, consistent with findings in other promoter targeted AhR ChIP-chip studies [33,35] (Lo *et al*., in submission). Moreover, relatively few alternative AhR response elements (5'-CATGN$_6$C[T|A]TG-3') [40,41] were identified in AhR enriched regions lacking a DRE core sequence. Enrichment in regions lacking DRE cores provides additional evidence of AhR-DNA interactions that don not involve the basic bHLH domain [63], such as tethering to other DNA interacting TFs and/or tertiary interactions with looping DNA.

Integration of gene expression, ChIP-chip, and DRE distribution data suggests that ~35% of all differentially expressed hepatic genes are mediated by direct AhR binding to a DRE. Consequently, 65% of the gene expression responses elicited by TCDD do not involve direct AhR binding to a DRE. However, TF binding analyses based on tiling arrays is limited by the extent of probe coverage (Figure 1). Genomic regions lacking probe coverage may falsely inflate the number of DRE-absent AhR enriched regions, thus underestimating the number of AhR regulated genes involving a DRE. Furthermore, the analyses may not be exhaustive due to the technical limitations of ChIP-chip assay coupled with the conservative FDR threshold used to identify statistically significant signals, which may have excluded some positive signals. These limitations of the technology could be addressed in ChIP-seq experiments, which have greater resolution and sensitivity [64,65]. The shorter sequence reads would improve resolution, but may also identify fewer regions containing a DRE. The higher sensitivity of ChIP-seq could also identify additional regions of AhR enrichment. ChIP-seq studies could also confirm AhR binding in these genomic regions in either a DRE-dependent or -independent manner.

TCDD induces hepatic vacuolization and lipid accumulation with differential gene expression associated with fatty acid metabolism and transport [25,53]. Independent functional annotation analysis of differentially expressed genes with significant AhR enrichment using DAVID and IPA identified over-represented processes related to fatty acid and lipid metabolism. Computational analysis also identified over-represented binding motifs for TFs involved in the regulation of lipid and cholesterol metabolism, including sites for HNF4, LXR, PXR, PPAR and COUP-TF. COUP-TF is a potent repressor that antagonizes transcriptional responses mediated by other nuclear receptors including HNF4, PPAR, ER, RAR and VDR [66]. For example, COUP-TF antagonizes HNF4α-mediated responses by binding HNF4α response elements [67-71]. Furthermore, AhR interactions with COUP-TF repress ER-mediated gene expression responses [47]. Therefore, AhR interactions with COUP-TF may regulate lipid and fatty acid metabolism by blocking HNF4α target gene expression (Figure 10A). Coincidentally, the HNF4 binding motif is over represented within AhR enriched regions lacking a DRE core.

Consistent with this proposed mechanism, several HNF4α regulated genes, including *Cyp7a1* and *Gck*, exhibited AhR enrichment and were repressed by

TCDD. Cyp7a1 is the rate-limiting enzyme in the bile acid biosynthetic pathway that converts cholesterol into bile acids. Transgenic mice over-expressing Cyp7a1 are protected from high-fat diet induced obesity, fatty liver and insulin resistance [72]. Moreover, a genetic deficiency of Cyp7a1 in humans results in hyperlipidemia [73]. Gck phosphorylates glucose in the initial step of glycolysis. Mutations in *Gck* that reduce kinase activity are associated with insulin resistance and maturity onset diabetes of young 2 (MODY2) in humans [74-76]. Furthermore, mice over-expressing Gck are resistant to MODY2 [77]. The down-regulation of *Cyp7a1* and *Gck*, possibly due to AhR - COUP-TF interactions at HNF4α response elements, is consistent TCDD-induced hepatic lipid accumulation in mice. Interestingly, TCDD exposure has been linked to diabetes and metabolic syndrome in humans [78-84]. Studies examining AhR-COUP-TF interactions and their effects on HNF4 target gene expression are being investigated further.

Conclusion

This study identified the genome-wide locations of TCDD-induced hepatic AhR enrichment *in vivo* and incorporates DRE distribution and differential gene expression data to further elucidate the hepatic AhR regulatory network. In addition to identifying interactions in regions associated with genes, AhR enrichment in distal non-coding intergenic regions was characterized. The functional significance of these distal interactions is unknown but intergenic binding has been reported for other TFs, and warrants further investigation. Moreover, only ~50% of all AhR enriched regions involved a DRE, suggesting that indirect AhR binding to DNA plays a significant role in the AhR regulatory network.

Methods

Animal Handling and Treatment

Hepatic tissue samples from immature female ovariectomized C57BL/6 mice obtained from a previous study [53] were used for both ChIP assays at 2 and 24 hrs, and gene expression analyses across all time points. Briefly, mice were orally gavaged with 30 μg/kg TCDD and sacrificed by cervical dislocation at 2, 4, 8, 12, 18, 24, 72 or 168 hrs postdose. Tissues were removed, weighed, and multiple samples (~100 mg each) were flash frozen in liquid nitrogen and stored at -80°C until further use.

Chromatin Immunoprecipitation (ChIP) and ChIP-chip Experiments

ChIP assays were performed as previously described [33] with the following changes. Approximately 100 mg of mouse liver was homogenized in 1% formaldehyde and incubated for 10 min at room temperature. Tissue homogenate was centrifuged at 10,000 RPM for 3 min at 4°C. Pellet was washed in ice-cold PBS, centrifuged, and resuspended in 900 μL of TSEI (20 mM Tris-HCl [pH 8.0], 150 mM NaCl, 2 mM EDTA, 1% Triton X-100, 0.1% sodium dodecyl sulfate) + 1× Protease Inhibitor Cocktail (Sigma, St. Louis, MO). Samples were sonicated 12 times for 10 s each time at 25% amplitude using a Branson 450 sonifier. Supernatant was transferred to fresh microcentrifuge tubes and incubated with rabbit IgG (5 μg; Sigma) and anti-AhR (5 μg; SA-210, Biomol) overnight at 4°C under gentle agitation. ChIP samples were washed and the DNA was isolated as previously described [33]. For ChIP-chip experiments, immunoprecipitated DNA isolated following immunoprecipitation with anti-AhR of liver extracts from TCDD-treated mice was linearly amplified using a whole genome amplification kit according to the manufacturer's instructions (Sigma). Linearly amplified DNA (7.5 μg) was fragmented by limited DNAseI digestion and hybridized to Affymetrix GeneChip® mouse 2.0R tiling arrays (Affymetrix, Santa Clara, CA) as previously described [33]. The hybridization and washing steps were performed according to the manufacturer's protocol at the Centre for Applied Genomics (Toronto, Canada). Data were normalized and analyzed using CisGenome and mapped against mouse genome version mm9 [36]. Enriched regions with a false discovery rate (FDR) of 1.0% (0.01) were determined by comparing triplicate samples of AhR_{TCDD} to triplicate IgG_{TCDD} using a moving average (MA) approach with default settings in TileMap v2 [85]. Regions were merged if the gap between them was < 300 bp and the number of probes failing to reach the cut-off was < 5. Regions were discarded if they were < 120 bp or did not contain at least 5 continuous probes above the cut-off. ChIPed DNA was purified using the PCR purification kit from BioBasic Inc. (Markham, ON) and quantified using quantitative real-time PCR (QRTPCR) (KAPA SYBR Fast qPCR Master Mix; KAPA Biosystems, Toronto, ON) (ChIP-PCR). Fold enrichment values were calculated relative to IgG controls. ChIP-PCR primer sequences are provided in Additional File 14.

ChIP-chip Location Analysis

The mouse genomic assembly (mm9) and associated annotation within the refGene and refLink databases were downloaded from the UCSC Genome Browser [86]. Individual segments of a gene region (i.e. the 10 kb sequence upstream of a TSS, the 5' and 3' UTRs and the CDS) for each mature gene encoding reference sequence (RefSeqs with NM prefixed identifiers) were determined using the genomic coordinates within the refGene databases (Additional File 3). Intragenic DNA regions within

the genomes were computationally identified by merging overlapping gene regions (Additional File 3) from both strands of the genome, and the DNA between adjacent intragenic regions are defined as the non-transcribed intergenic DNA regions (Additional File 3). AhR enrichment densities were calculated based on the number of significant enriched regions occurring in an interrogated region (e.g. intergenic DNA region or 5' UTR) divided by the total sum of the region length. Gene annotation associated with each RefSeq sequence was derived from the refLink database in the UCSC Genome Browser.

Transcription Factor Motif Analysis

The locations of AhR enrichment were compared against 5'-GCGTG-3' DRE core sequence locations in the mouse genome [8]. Identification of TF motifs over-represented in regions containing a DRE core were performed using the default parameter settings in RegionMiner, a program within the Genomatix suite of applications http://www.genomatix.de that contains an extensive database of TF binding motifs. Identified module families and individual matrices with z-scores > 3 were considered significant [87]. *De novo* motif discovery was performed using the Gibbs motif sampler in CisGenome on AhR regions of enrichment sequences not containing a DRE. Matrices for over-represented motifs were compared to existing TF binding motifs in JASPAR and TRANSFAC [48,49] using STAMP [50].

Comparison with Microarray Gene Expression

Results from the ChIP-chip and DRE analysis were integrated with whole-genome gene expression profiling data from mice orally gavaged with 30 μg/kg TCDD using 4 × 44 k whole-genome oligonucleotide arrays from Agilent Technologies (Santa Clara, CA) [8]. The genomic locations of the differentially responsive genes (|fold change| ≥ 1.5 and P1(t) > 0.999) were obtained for each RefSeq sequence associated with the gene from the refGene database in the UCSC Genome Browser. Circos plots [88] were generated to visualize the locations of DRE cores, regions of AhR enrichment and temporal heatmaps of temporal gene expression responses.

Functional Annotation and Pathway Analysis

Functional annotation clustering of Gene Ontology (GO) terms for genes associated with significant AhR enrichment was performed using DAVID (Database for Annotation, Visualization, and Integrated Discovery) [51]. In addition, the regions were analyzed using Ingenuity Pathway Analysis (IPA; http://www.ingenuity.com/) to identify over-represented molecular and cellular functions based on the Fisher's Exact Test p-value < 0.01.

Additional material

Additional file 1: Genomic location, gene annotation and enrichment values of significant (FDR < 0.01) TCDD-induced AhR enrichment at 2 hrs. Detailed results of the AhR ChIP-chip analysis that include the genomic location and TCDD-induced enrichment values, and the gene annotation of enrichment peaks located within the 10 kb upstream and transcribed region of a gene.

Additional file 2: Genomic location, gene annotation and enrichment values of significant (FDR < 0.01) TCDD-induced AhR enrichment at 24 hrs. Detailed results of the AhR ChIP-chip analysis that include the genomic location and TCDD-induced enrichment values, and the gene annotation of enrichment peaks located within the 10 kb upstream and transcribed region of a gene.

Additional file 3: Definitions of various genomic regions used to map regions of AhR enrichment. **A)** Genomic locations from the UCSC Genome Browser refGene database were used to obtain sequences for 10 kb region upstream of the TSS, the 5' and 3' UTRs, and the CDS of every known human, mouse and rat RefSeq sequence. A gene region is defined as the sequence spanning the region 10 kb upstream of a TSS through to the end of the 3' UTR. **B)** Intragenic DNA regions in a genome were determined by combining the non-overlapping gene regions. For example, gene regions of tissue specific isoforms of a gene that have different TSS positions were merged to determine the longest spanning range (genes C & C' and genes E & E'). Additionally, overlapping genes on both strands of the genome were also merged (genes B + E + E'). Non-transcribed DNA segments that span the regions between adjacent intragenic regions are defined as the intergenic DNA regions.

Additional file 4: TCDD-induced AhR enrichment (FDR < 0.01) density across the mouse genome at 2 hrs. The density of significant AhR enrichment (per Mbp) at 2 hrs were calculated for each of the defined genomic regions across the individual chromosomes.

Additional file 5: TCDD-induced AhR enrichment (FDR < 0.01) density across the mouse genome at 24 hrs. The density of significant AhR enrichment (per Mbp) at 24 hrs were calculated for each of the defined genomic regions across the individual chromosomes.

Additional file 6: Transcription factor binding site analysis of significant TCDD-induced AhR enrichment (FDR < 0.01) at 2 hrs. DNA sequences for the regions of significant AhR enrichment at 2 hrs were analyzed for transcription factor (TF) binding site motif over-representation using RegionMiner. The results list the TF matrices and their corresponding over-representation and z-score value.

Additional file 7: Transcription factor binding site analysis of significant TCDD-induced AhR enrichment (FDR < 0.01) at 24 hrs. DNA sequences for the regions of significant AhR enrichment at 24 hrs were analyzed for transcription factor (TF) binding site motif over-representation using RegionMiner. The results list the TF matrices and their corresponding over-representation and z-score value.

Additional file 8: Over-representation of transcription factor binding motifs located proximally (10-50 bp) of a DRE in a significantly AhR enriched region (FDR < 0.01). DNA sequences for the regions of significant AhR enrichment at 2 and 24 hrs possessing a DRE core sequence (5'-GCGTG-3') were analyzed for transcription factor (TF) binding site motif over-representation using RegionMiner. The results list the TF matrices and their corresponding over-representation and z-score value.

Additional file 9: Repetitive sequence elements identified in the *de novo* motif analysis of significant intragenic and intergenic AhR enriched regions (FDR < 0.01) lacking a DRE core. The repetitive over-represented motifs from each region are shown with their consensus and reverse complement sequence, and the Gibbs motif sampler score.

Additional file 10: Pathway analysis of genes associated with DRE-containing regions of AhR enrichment (FDR < 0.01) at 2 hrs. List of the most significant Bio-Functions (p < 0.01) identified using Ingenuity Pathway Analysis for the genes associated with a significant AhR

enriched region (FDR < 0.01) containing a DRE core (5'-GCGTG-3') at 2 hrs.

Additional file 11: Pathway analysis of genes associated with DRE-containing regions of AhR enrichment (FDR < 0.01) at 24 hrs. List of the most significant Bio-Functions (p < 0.01) identified using Ingenuity Pathway Analysis for the genes associated with a significant AhR enriched region (FDR < 0.01) containing a DRE core (5'-GCGTG-3') at 24 hrs.

Additional file 12: Circos plots integrating DRE analysis, AhR enrichment (2 hrs; FDR < 0.01) and heatmaps for hepatic differential gene expression responses (|fold change| ≥ 1.5 and P1 (t) > 0.999) induced by TCDD across the genome. Circos plots illustrate the ideograms for each individual chromosome and the entire genome and integrate the results of the DRE, ChIP-chip and gene expression analyses.

Additional file 13: Pathway analysis of differentially regulated genes (|fold change| ≥ 1.5 and P1(t) > 0.999) associated with regions of AhR enrichment (FDR < 0.01) at 2 hrs. List of the most significant Bio-Functions (p < 0.01) identified using Ingenuity Pathway Analysis for TCDD-elicited gene expression responses (|fold change| ≥ 1.5 and P1(t) > 0.999) associated with a significant AhR enriched region (FDR < 0.01) containing a DRE core (5'-GCGTG-3') at 24 hrs.

Additional file 14: Primer sequences used to verify 2 hr ChIP-chip responses. QRTPCR primers used to verify AhR enriched regions isolated from the 2 hr ChIP-chip.

Acknowledgements
This work was supported by the National Institute of Environmental Health Sciences Superfund Basic Research Program [P42ES04911 to TRZ] and by the Canadian Institute of Health Research [MOP-82715 to JM]. JM is a recipient of the Canadian Institute of Health Research New Investigator Award. TRZ is partially supported by the Michigan Agricultural Extension Station.

Author details
[1]Department of Biochemistry & Molecular Biology, Michigan State University, East Lansing, MI, 48824, USA. [2]Department of Pharmacology & Toxicology, University of Toronto, Toronto, Ontario, M5S 1A8, Canada. [3]Center for Integrative Toxicology, Michigan State University, East Lansing, MI, 48824, USA.

Authors' contributions
ED performed the computational analyses and integration of the ChIP-chip data with the computational DRE and microarray gene expression analyses, and the initial preparation of the manuscript. JM optimized and performed the ChIP experiments, and normalized the ChIP-chip data. TL and RL validated the ChIP-chip results with ChIP-PCR from regions identified by ED. TRZ oversaw the completion of the study. All the authors have given final approval of the version to be published.

Received: 17 September 2010 Accepted: 15 July 2011
Published: 15 July 2011

References
1. Gu Y, Hogenesch J, Bradfield C: **The PAS superfamily: sensors of environmental and developmental signals.** *Annu Rev Pharmacol Toxicol* 2000, **40**:519-561.
2. Denison MS, Heath-Pagliuso S: **The Ah receptor: a regulator of the biochemical and toxicological actions of structurally diverse chemicals.** *Bulletin of environmental contamination and toxicology* 1998, **61**:557-568.
3. Poland A, Knutson JC: **2,3,7,8-tetrachlorodibenzo-p-dioxin and related halogenated aromatic hydrocarbons: examination of the mechanism of toxicity.** *Annu Rev Pharmacol Toxicol* 1982, **22**:517-554.
4. Hankinson O: **The aryl hydrocarbon receptor complex.** *Annu Rev Pharmacol Toxicol* 1995, **35**:307-340.
5. Okey AB, Vella LM, Harper PA: **Detection and characterization of a low affinity form of cytosolic Ah receptor in livers of mice nonresponsive to induction of cytochrome P1-450 by 3-methylcholanthrene.** *Molecular Pharmacology* 1989, **35**:823-830.
6. Gonzalez F, Fernandez-Salguero P: **The aryl hydrocarbon receptor: studies using the AHR-null mice.** *Drug Metab Dispos* 1998, **26**:1194-1198.
7. Swanson H, Chan W, Bradfield C: **DNA binding specificities and pairing rules of the Ah receptor, ARNT, and SIM proteins.** *J Biol Chem* 1995, **270**:26292-26302.
8. Dere E, Forgacs AL, Zacharewski TR, Burgoon LD: **Genome-Wide Computational Analysis of Dioxin Response Element Location and Distribution in the Human, Mouse, and Rat Genomes.** *Chem Res Toxicol* 2011.
9. Farnham PJ: **Insights from genomic profiling of transcription factors.** *Nat Rev Genet* 2009, **10**:605-616.
10. Carroll JS, Meyer CA, Song J, Li W, Geistlinger TR, Eeckhoute J, Brodsky AS, Keeton EK, Fertuck KC, Hall GF, *et al*: **Genome-wide analysis of estrogen receptor binding sites.** *Nature Genetics* 2006, **38**:1289-1297.
11. Carroll JS, Liu XS, Brodsky AS, Li W, Meyer CA, Szary AJ, Eeckhoute J, Shao W, Hestermann EV, Geistlinger TR, *et al*: **Chromosome-wide mapping of estrogen receptor binding reveals long-range regulation requiring the forkhead protein FoxA1.** *Cell* 2005, **122**:33-43.
12. Deblois G, Hall JA, Perry M-C, Laganière J, Ghahremani M, Park M, Hallett M, Giguère V: **Genome-wide identification of direct target genes implicates estrogen-related receptor alpha as a determinant of breast cancer heterogeneity.** *Cancer Res* 2009, **69**:6149-6157.
13. Laganière J, Deblois G, Lefebvre C, Bataille AR, Robert F, Giguère V: **From the Cover: Location analysis of estrogen receptor alpha target promoters reveals that FOXA1 defines a domain of the estrogen response.** *Proc Natl Acad Sci USA* 2005, **102**:11651-11656.
14. Lin C-Y, Vega VB, Thomsen JS, Zhang T, Kong SL, Xie M, Chiu KP, Lipovich L, Barnett DH, Stossi F, *et al*: **Whole-genome cartography of estrogen receptor alpha binding sites.** *PLoS Genet* 2007, **3**:e87.
15. van der Meer DLM, Degenhardt T, Väisänen S, de Groot PJ, Heinäniemi M, de Vries SC, Müller M, Carlberg C, Kersten S: **Profiling of promoter occupancy by PPARalpha in human hepatoma cells via ChIP-chip analysis.** *Nucleic Acids Res* 2010, **38**:2839-2850.
16. Chong HK, Infante AM, Seo Y-K, Jeon T-I, Zhang Y, Edwards PA, Xie X, Osborne TF: **Genome-wide interrogation of hepatic FXR reveals an asymmetric IR-1 motif and synergy with LRH-1.** *Nucleic acids research* 2010.
17. Wederell ED, Bilenky M, Cullum R, Thiessen N, Dagpinar M, Delaney A, Varhol R, Zhao Y, Zeng T, Bernier B, *et al*: **Global analysis of in vivo Foxa2-binding sites in mouse adult liver using massively parallel sequencing.** *Nucleic Acids Res* 2008, **36**:4549-4564.
18. Wei G-H, Badis G, Berger MF, Kivioja T, Palin K, Enge M, Bonke M, Jolma A, Varjosalo M, Gehrke AR, *et al*: **Genome-wide analysis of ETS-family DNA-binding in vitro and in vivo.** *The EMBO journal* 2010.
19. Malhotra D, Portales-Casamar E, Singh A, Srivastava S, Arenillas D, Happel C, Shyr C, Wakabayashi N, Kensler TW, Wasserman WW, Biswal S: **Global mapping of binding sites for Nrf2 identifies novel targets in cell survival response through ChIP-Seq profiling and network analysis.** *Nucleic acids research* 2010.
20. Schmidt D, Wilson MD, Ballester B, Schwalie PC, Brown GD, Marshall A, Kutter C, Watt S, Martinez-Jimenez CP, Mackay S, *et al*: **Five-vertebrate ChIP-seq reveals the evolutionary dynamics of transcription factor binding.** *Science* 2010, **328**:1036-1040.
21. Ramos YFM, Hestand MS, Verlaan M, Krabbendam E, Ariyurek Y, van Galen M, van Dam H, van Ommen G-JB, den Dunnen JT, Zantema A, 't Hoen PAC: **Genome-wide assessment of differential roles for p300 and CBP in transcription regulation.** *Nucleic acids research* 2010.
22. Gupta R, Wikramasinghe P, Bhattacharyya A, Perez FA, Pal S, Davuluri RV: **Annotation of gene promoters by integrative data-mining of ChIP-seq Pol-II enrichment data.** *BMC Bioinformatics* 2010, **11(Suppl 1)**:S65.
23. Tallack MR, Whitington T, Shan Yuen W, Wainwright EN, Keys JR, Gardiner BB, Nourbakhsh E, Cloonan N, Grimmond SM, Bailey TL, Perkins AC: **A global role for KLF1 in erythropoiesis revealed by ChIP-seq in primary erythroid cells.** *Genome research* 2010.
24. Consortium EP, Birney E, Stamatoyannopoulos JA, Dutta A, Guigó R, Gingeras TR, Margulies EH, Weng Z, Snyder M, Dermitzakis ET, *et al*: **Identification and analysis of functional elements in 1% of the human genome by the ENCODE pilot project.** *Nature* 2007, **447**:799-816.
25. Boverhof DR, Burgoon LD, Tashiro C, Sharratt B, Chittim B, Harkema JR, Mendrick DL, Zacharewski TR: **Comparative toxicogenomic analysis of the**

hepatotoxic effects of TCDD in Sprague Dawley rats and C57BL/6 mice. *Toxicol Sci* 2006, **94**:398-416.
26. Dere E, Boverhof DR, Burgoon LD, Zacharewski TR: **In vivo-in vitro toxicogenomic comparison of TCDD-elicited gene expression in Hepa1c1c7 mouse hepatoma cells and C57BL/6 hepatic tissue.** *BMC Genomics* 2006, **7**:80.
27. Puga A, Maier A, Medvedovic M: **The transcriptional signature of dioxin in human hepatoma HepG2 cells.** *Biochem Pharmacol* 2000, **60**:1129-1142.
28. Hayes K, Zastrow G, Nukaya M, Pande K, Glover E, Maufort J, Liss A, Liu Y, Moran S, Vollrath A, Bradfield C: **Hepatic transcriptional networks induced by exposure to 2,3,7,8-tetrachlorodibenzo-p-dioxin.** *Chem Res Toxicol* 2007, **20**:1573-1581.
29. Boutros PC, Yan R, Moffat ID, Pohjanvirta R, Okey AB: **Transcriptomic responses to 2,3,7,8-tetrachlorodibenzo-p-dioxin (TCDD) in liver: comparison of rat and mouse.** *BMC Genomics* 2008, **9**:419.
30. Flaveny CA, Murray IA, Perdew GH: **Differential gene regulation by the human and mouse aryl hydrocarbon receptor.** *Toxicological sciences: an official journal of the Society of Toxicology* 2010, **114**:217-225.
31. Whitlock J: **Induction of cytochrome P4501A1.** *Annu Rev Pharmacol Toxicol* 1999, **39**:103-125.
32. Ahmed S, Valen E, Sandelin A, Matthews J: **Dioxin increases the interaction between aryl hydrocarbon receptor and estrogen receptor alpha at human promoters.** *Toxicol Sci* 2009, **111**:254-266.
33. Pansoy A, Ahmed S, Valen E, Sandelin A, Matthews J: **3-methylcholanthrene induces differential recruitment of aryl hydrocarbon receptor to human promoters.** *Toxicological sciences: an official journal of the Society of Toxicology* 2010.
34. Sartor MA, Schnekenburger M, Marlowe JL, Reichard JF, Wang Y, Fan Y, Ma C, Karyala S, Halbleib D, Liu X, *et al*: **Genomewide analysis of aryl hydrocarbon receptor binding targets reveals an extensive array of gene clusters that control morphogenetic and developmental programs.** *Environ Health Perspect* 2009, **117**:1139-1146.
35. Kinehara M, Fukuda I, Yoshida K-I, Ashida H: **High-throughput evaluation of aryl hydrocarbon receptor-binding sites selected via chromatin immunoprecipitation-based screening in Hepa-1c1c7 cells stimulated with 2,3,7,8-tetrachlorodibenzo-p-dioxin.** *Genes Genet Syst* 2008, **83**:455-468.
36. Ji H, Jiang H, Ma W, Johnson DS, Myers RM, Wong WH: **An integrated software system for analyzing ChIP-chip and ChIP-seq data.** *Nat Biotechnol* 2008, **26**:1293-1300.
37. Ma Q, Baldwin K: **2,3,7,8-tetrachlorodibenzo-p-dioxin-induced degradation of aryl hydrocarbon receptor (AhR) by the ubiquitin-proteasome pathway. Role of the transcription activaton and DNA binding of AhR.** *J Biol Chem* 2000, **275**:8432-8438.
38. Pollenz RS: **The mechanism of AH receptor protein down-regulation (degradation) and its impact on AH receptor-mediated gene regulation.** *Chem Biol Interact* 2002, **141**:41-61.
39. Song Z, Pollenz R: **Ligand-dependent and independent modulation of aryl hydrocarbon receptor localization, degradation, and gene regulation.** *Mol Pharmacol* 2002, **62**:806-816.
40. Boutros PC, Moffat ID, Franc MA, Tijet N, Tuomisto J, Pohjanvirta R, Okey AB: **Dioxin-responsive AHRE-II gene battery: identification by phylogenetic footprinting.** *Biochem Biophys Res Commun* 2004, **321**:707-715.
41. Sogawa K, Numayama-Tsuruta K, Takahashi T, Matsushita N, Miura C, Nikawa J-i, Gotoh O, Kikuchi Y, Fujii-Kuriyama Y: **A novel induction mechanism of the rat CYP1A2 gene mediated by Ah receptor-Arnt heterodimer.** *Biochem Biophys Res Commun* 2004, **318**:746-755.
42. Richter K, Nessling M, Lichter P: **Macromolecular crowding and its potential impact on nuclear function.** *Biochim Biophys Acta* 2008, **1783**:2100-2107.
43. Li G-W, Berg OG, Elf J: **Effects of macromolecular crowding and DNA looping on gene regulation kinetics.** *Nature Physics* 2009, **5**:294.
44. Kobayashi A, Sogawa K, Fujii-Kuriyama Y: **Cooperative interaction between AhR.Arnt and Sp1 for the drug-inducible expression of CYP1A1 gene.** *The Journal of biological chemistry* 1996, **271**:12310-12316.
45. Dabir P, Marinic TE, Krukovets I, Stenina OI: **Aryl hydrocarbon receptor is activated by glucose and regulates the thrombospondin-1 gene promoter in endothelial cells.** *Circ Res* 2008, **102**:1558-1565.
46. Marlowe J, Fan Y, Chang X, Peng L, Knudsen E, Xia Y, Puga A: **The aryl hydrocarbon receptor binds to E2F1 and inhibits E2F1-induced apoptosis.** *Mol Biol Cell* 2008, **19**:3263-3271.
47. Klinge CM, Kaur K, Swanson HI: **The aryl hydrocarbon receptor interacts with estrogen receptor alpha and orphan receptors COUP-TFI and ERRalpha1.** *Arch Biochem Biophys* 2000, **373**:163-174.
48. Portales-Casamar E, Thongjuea S, Kwon AT, Arenillas D, Zhao X, Valen E, Yusuf D, Lenhard B, Wasserman WW, Sandelin A: **JASPAR 2010: the greatly expanded open-access database of transcription factor binding profiles.** *Nucleic Acids Research* 2010, **38**:D105-110.
49. Matys V, Fricke E, Geffers R, Gössling E, Haubrock M, Hehl R, Hornischer K, Karas D, Kel AE, Kel-Margoulis OV, *et al*: **TRANSFAC: transcriptional regulation, from patterns to profiles.** *Nucleic Acids Res* 2003, **31**:374-378.
50. Mahony S, Auron PE, Benos PV: **DNA familial binding profiles made easy: comparison of various motif alignment and clustering strategies.** *PLoS Comput Biol* 2007, **3**:e61.
51. Dennis G, Sherman BT, Hosack DA, Yang J, Gao W, Lane HC, Lempicki RA: **DAVID: Database for Annotation, Visualization, and Integrated Discovery.** *Genome Biol* 2003, **4**:P3.
52. Kopec AK, Boverhof DR, Burgoon LD, Ibrahim-Aibo D, Harkema JR, Tashiro C, Chittim B, Zacharewski TR: **Comparative toxicogenomic examination of the hepatic effects of PCB126 and TCDD in immature, ovariectomized C57BL/6 mice.** *Toxicol Sci* 2008, **102**:61-75.
53. Boverhof DR, Burgoon LD, Tashiro C, Chittim B, Harkema JR, Jump DB, Zacharewski TR: **Temporal and dose-dependent hepatic gene expression patterns in mice provide new insights into TCDD-Mediated hepatotoxicity.** *Toxicol Sci* 2005, **85**:1048-1063.
54. Köhle C, Bock KW: **Coordinate regulation of Phase I and II xenobiotic metabolisms by the Ah receptor and Nrf2.** *Biochemical Pharmacology* 2007, **73**:1853-1862.
55. Nioi P, Hayes JD: **Contribution of NAD(P)H:quinone oxidoreductase 1 to protection against carcinogenesis, and regulation of its gene by the Nrf2 basic-region leucine zipper and the arylhydrocarbon receptor basic helix-loop-helix transcription factors.** *Mutation research* 2004, **555**:149-171.
56. Yeager RL, Reisman SA, Aleksunes LM, Klaassen CD: **Introducing the "TCDD-inducible AhR-Nrf2 gene battery".** *Toxicological sciences: an official journal of the Society of Toxicology* 2009, **111**:238-246.
57. De Abrew KN, Kaminski NE, Thomas RS: **An integrated genomic analysis of aryl hydrocarbon receptor-mediated inhibition of B-cell differentiation.** *Toxicological sciences: an official journal of the Society of Toxicology* 2010, **118**:454-469.
58. Hamza MS, Pott S, Vega VB, Thomsen JS, Kandhadayar GS, Ng PWP, Chiu KP, Pettersson S, Wei CL, Ruan Y, Liu ET: **De-novo identification of PPARgamma/RXR binding sites and direct targets during adipogenesis.** *PLoS ONE* 2009, **4**:e4907.
59. O'Geen H, Squazzo SL, Iyengar S, Blahnik K, Rinn JL, Chang HY, Green R, Farnham PJ: **Genome-wide analysis of KAP1 binding suggests autoregulation of KRAB-ZNFs.** *PLoS Genet* 2007, **3**:e89.
60. Xu X, Bieda M, Jin VX, Rabinovich A, Oberley MJ, Green R, Farnham PJ: **A comprehensive ChIP-chip analysis of E2F1, E2F4, and E2F6 in normal and tumor cells reveals interchangeable roles of E2F family members.** *Genome research* 2007, **17**:1550-1561.
61. Li Q, Barkess G, Qian H: **Chromatin looping and the probability of transcription.** *Trends Genet* 2006, **22**:197-202.
62. Long X, Miano JM: **Remote control of gene expression.** *J Biol Chem* 2007, **282**:15941-15945.
63. Murray IA, Morales JL, Flaveny CA, Dinatale BC, Chiaro C, Gowdahalli K, Amin S, Perdew GH: **Evidence for ligand-mediated selective modulation of aryl hydrocarbon receptor activity.** *Molecular Pharmacology* 2010, **77**:247-254.
64. Gilchrist DA, Fargo DC, Adelman K: **Using ChIP-chip and ChIP-seq to study the regulation of gene expression: genome-wide localization studies reveal widespread regulation of transcription elongation.** *Methods* 2009, **48**:398-408.
65. Liu ET, Pott S, Huss M: **Q&A: ChIP-seq technologies and the study of gene regulation.** *BMC Biology* 2010, **8**:56.
66. Giguère V: **Orphan nuclear receptors: from gene to function.** *Endocr Rev* 1999, **20**:689-725.
67. Viollet B, Kahn A, Raymondjean M: **Protein kinase A-dependent phosphorylation modulates DNA-binding activity of hepatocyte nuclear factor 4.** *Molecular and Cellular Biology* 1997, **17**:4208-4219.
68. Mietus-Snyder M, Sladek FM, Ginsburg GS, Kuo CF, Ladias JA, Darnell JE, Karathanasis SK: **Antagonism between apolipoprotein AI regulatory protein 1, Ear3/COUP-TF, and hepatocyte nuclear factor 4 modulates**

apolipoprotein CIII gene expression in liver and intestinal cells. *Molecular and Cellular Biology* 1992, **12**:1708-1718.
69. Ladias JA, Hadzopoulou-Cladaras M, Kardassis D, Cardot P, Cheng J, Zannis V, Cladaras C: **Transcriptional regulation of human apolipoprotein genes ApoB, ApoCIII, and ApoAII by members of the steroid hormone receptor superfamily HNF-4, ARP-1, EAR-2, and EAR-3.** *The Journal of biological chemistry* 1992, **267**:15849-15860.
70. Pineda Torra I, Jamshidi Y, Flavell D, Fruchart J-C, Staels B: **Characterization of the Human PPAR{alpha} Promoter: Identification of a Functional Nuclear Receptor Response Element.** *Molecular Endocrinology* 2002, **16**:1013.
71. You M, Fischer M, Cho WK, Crabb D: **Transcriptional control of the human aldehyde dehydrogenase 2 promoter by hepatocyte nuclear factor 4: inhibition by cyclic AMP and COUP transcription factors.** *Arch Biochem Biophys* 2002, **398**:79-86.
72. Li T, Owsley E, Matozel M, Hsu P, Novak CM, Chiang JYL: **Transgenic expression of cholesterol 7alpha-hydroxylase in the liver prevents high-fat diet-induced obesity and insulin resistance in mice.** *Hepatology* 2010, **52**:678-690.
73. Pullinger CR, Eng C, Salen G, Shefer S, Batta AK, Erickson SK, Verhagen A, Rivera CR, Mulvihill SJ, Malloy MJ, Kane JP: **Human cholesterol 7alpha-hydroxylase (CYP7A1) deficiency has a hypercholesterolemic phenotype.** *J Clin Invest* 2002, **110**:109-117.
74. Caro JF, Triester S, Patel VK, Tapscott EB, Frazier NL, Dohm GL: **Liver glucokinase: decreased activity in patients with type II diabetes.** *Horm Metab Res* 1995, **27**:19-22.
75. Stoffel M, Froguel P, Takeda J, Zouali H, Vionnet N, Nishi S, Weber IT, Harrison RW, Pilkis SJ, Lesage S: **Human glucokinase gene: isolation, characterization, and identification of two missense mutations linked to early-onset non-insulin-dependent (type 2) diabetes mellitus.** *Proc Natl Acad Sci USA* 1992, **89**:7698-7702.
76. Marks SD, Couch RM: **Identification of two new mutations in the glucokinase gene that result in maturity-onset diabetes of the young.** *Diabetes Care* 2010, **33**:e94.
77. Shiota M, Postic C, Fujimoto Y, Jetton TL, Dixon K, Pan D, Grimsby J, Grippo JF, Magnuson MA, Cherrington AD: **Glucokinase gene locus transgenic mice are resistant to the development of obesity-induced type 2 diabetes.** *Diabetes* 2001, **50**:622-629.
78. Angulo P: **Nonalcoholic fatty liver disease.** *N Engl J Med* 2002, **346**:1221-1231.
79. Kang HK, Dalager NA, Needham LL, Patterson DG, Lees PSJ, Yates K, Matanoski GM: **Health status of Army Chemical Corps Vietnam veterans who sprayed defoliant in Vietnam.** *Am J Ind Med* 2006, **49**:875-884.
80. Jones OAH, Maguire ML, Griffin JL: **Environmental pollution and diabetes: a neglected association.** *Lancet* 2008, **371**:287-288.
81. Remillard RBJ, Bunce NJ: **Linking dioxins to diabetes: epidemiology and biologic plausibility.** *Environ Health Perspect* 2002, **110**:853-858.
82. Cranmer M, Louie S, Kennedy R, Kern P, Fonseca V: **Exposure to 2,3,7,8-Tetrachlorodibenzo-p-dioxin (TCDD) Is Associated with Hyperinsulinemia and Insulin Resistance.** *Toxicological Sciences* 2000, **56**:431.
83. Bertazzi PA, Bernucci I, Brambilla G, Consonni D, Pesatori AC: **The Seveso studies on early and long-term effects of dioxin exposure: a review.** *Environ Health Perspect* 1998, **106(Suppl 2)**:625-633.
84. Henriksen GL, Ketchum NS, Michalek JE, Swaby JA: **Serum dioxin and diabetes mellitus in veterans of Operation Ranch Hand.** *Epidemiology* 1997, **8**:252-258.
85. Ji H, Wong W: **TileMap: create chromosomal map of tiling array hybridizations.** *Bioinformatics* 2005, **21**:3629.
86. Rhead B, Karolchik D, Kuhn R, Hinrichs A, Zweig A, Fujita P, Diekhans M, Smith K, Rosenbloom K, Raney B, *et al*: **The UCSC Genome Browser database: update 2010.** *Nucleic Acids Research* 2010, **38**:D613.
87. Gerstman BB: *Basic Biostatistics: Statistics for Public Health Practice*. 1 edition. Sudbury, MA: Jones & Bartlett Publishers, Inc.; 2007.
88. Krzywinski M, Schein J, Birol I, Connors J, Gascoyne R, Horsman D, Jones SJ, Marra MA: **Circos: an information aesthetic for comparative genomics.** *Genome research* 2009, **19**:1639-1645.

doi:10.1186/1471-2164-12-365
Cite this article as: Dere *et al.*: Integration of Genome-Wide Computation DRE Search, AhR ChIP-chip and Gene Expression Analyses of TCDD-Elicited Responses in the Mouse Liver. *BMC Genomics* 2011 **12**:365.